applied sciences

MDPI

Systematic Review

Multi-Agent Systems for Decentralized Control and Management of Active Power Grid Peripheries: A Systematic Review

Sultan Mamun [1], Stelios Ioannou [2,3,*], Nicholas G. Christofides [4] and Mohamed Darwish [5]

1 School of Mechanical Engineering, Yangzhou University, Yangzhou 225009, China; ibfmamun@gmail.com
2 School of Sciences, University of Lancashire (UCLan), Larnaka 7080, Cyprus
3 Interdisciplinary Science Promotion & Innovative Research Exploration (INSPIRE) Research Centre, Larnaka 7080, Cyprus
4 Department of Electrical Engineering, Computer Engineering and Informatics, Frederick University, Nicosia 1036, Cyprus; n.christofides@frederick.ac.cy
5 Power Electronics and Systems, Department of Electronic and Computer Engineering, College of Engineering, Design and Physical Sciences, Brunel University London, London UB8 3PH, UK; mohamed.darwish@brunel.ac.uk
* Correspondence: sioannou2@uclan.ac.uk

Abstract

The transition from centralized fossil fuel-based power systems toward decentralized smart grids with a high penetration of renewable energy sources (RES) introduces substantial challenges in monitoring, control, coordination, and management. These challenges are particularly evident at the active power grid periphery, defined in this work as the decentralized edge layer of modern power systems comprising low-voltage distribution networks, distributed energy resources (DERs), prosumers, energy storage systems, electric vehicles (EVs), and localized intelligent control entities operating near the consumer side of the grid. This review systematically examines the role of multi-agent systems (MASs) in addressing these emerging challenges. A total of 160 articles, drawn predominantly from top-tier Q1 journals and published up to March 2026, were systematically analyzed to evaluate recent methodological advances, identify persistent research gaps, and compare existing problem formulations and mathematical techniques. The review covers MAS-based applications including distributed energy management, voltage and frequency regulation, demand-side management, microgrid coordination, EV charging coordination, resilience enhancement, and cyber-physical supervisory control. The findings indicate that although MASs offer enhanced scalability, flexibility, resilience, and decentralized decision-making capabilities, existing approaches continue to face significant limitations associated with communication latency, cybersecurity vulnerabilities, interoperability constraints, heterogeneous agent dynamics, and limited real-time experimental validation. Furthermore, this review proposes six emerging research hypotheses targeting underexplored domains, presents a methodological decision flowchart for MAS implementation and selection, and discusses future research directions involving the integration of digital twins, blockchain technologies, edge intelligence, and advanced communication architectures with MAS frameworks.

Keywords: active power grid periphery; multi-agent systems (MASs); smart grid; distributed energy resources; decentralized control; renewable energy systems; power systems

Check for updates

Academic Editor: Alexander Barkalov

Received: 20 May 2026
Revised: 23 June 2026
Accepted: 29 June 2026
Published: 8 July 2026

1. Introduction

1.1. Motivation

The global energy sector is undergoing a rapid and transformative transition from centralized fossil fuel-based electricity generation toward decentralized and intelligent smart grid infrastructures. By the year 2025, renewable energy sources (RES) accounted for more than 40% of global electricity generation [1,2]. Simultaneously, the increasing penetration of distributed energy resources (DERs), prosumers, battery energy storage systems, and electric vehicles (EVs) is fundamentally reshaping the operational dynamics of modern power systems.

Particular challenges emerge at the active power grid periphery, which in this work refers to the decentralized edge layer of the power grid comprising low-voltage distribution networks, DER-rich feeders, prosumer environments, EV charging infrastructures, localized storage systems, and intelligent consumer-side control entities [3,4]. Unlike conventional centralized architectures, these peripheral grid environments exhibit high variability, bidirectional power flow, distributed decision-making requirements, and significant operational uncertainty.

Traditional centralized control and supervisory frameworks are increasingly unable to effectively manage these highly dynamic and distributed environments due to limitations associated with scalability, communication latency, computational burden, and vulnerability to single points of failure [5–7]. Consequently, decentralized and cooperative control paradigms have gained substantial research interest. Among these emerging solutions, multi-agent systems (MASs) have attracted considerable attention as a promising framework for distributed monitoring, control, coordination, and management within modern smart grids [8,9]. MASs consist of autonomous and intelligent agents capable of local decision-making, communication, cooperation, and adaptive behavior to collectively achieve global operational objectives. Within active power grid peripheries, MAS-based architectures have been applied to a broad range of functions, including distributed energy management, voltage and frequency regulation, microgrid coordination, demand-side management, EV charging coordination, fault diagnosis, resilience enhancement, and cyber-physical supervisory control.

Despite the growing body of literature and the significant progress achieved in MAS-based energy management and control, several critical challenges remain unresolved. Existing approaches continue to face issues related to unreliable communication infrastructures [10], vulnerability to cyber-physical attacks [11], heterogeneous and nonlinear agent dynamics [12], interoperability limitations, and the absence of standardized benchmarking and validation frameworks [13]. Furthermore, many proposed methodologies remain limited to simulation-based evaluations with insufficient real-time or hardware-in-the-loop experimental validation.

Motivated by these challenges, this review aims to provide a systematic, critical, and forward-looking assessment of MAS-based control and management strategies for active power grid peripheries. In contrast to previous review studies, this work not only analyzes recent methodological developments and mathematical formulations but also systematically compares MAS architectures with hierarchical industrial control frameworks based on IEC 61850 standards [14]. Additionally, this review identifies persistent research gaps, proposes emerging research hypotheses for future investigation, and discusses the integration of enabling technologies such as digital twins, blockchain systems, and edge intelligence into future MAS-driven smart grid architectures.

https://doi.org/10.3390/app16146863

1.2. Contributions

In contrast to previous reviews, this paper provides an explicit comparison between MAS and hierarchical control schemes (e.g., IEC 61850-based [14] centralized and decentralized architectures), which continue to serve as the industry benchmark. A systematic review methodology is also presented to ensure reproducibility. First, the paper reviews contemporary multi-agent system (MAS) approaches for the control and management of the active grid periphery, synthesizing findings from 160 top-tier Q1 journal articles published up to March 2026. The unique contributions of this review are summarized in Table 1.

Table 1. Unique contributions of this review.

Contribution Area	Specific Novelty
Scope	First review to explicitly focus on the active power grid periphery and provide a systematic comparison against hierarchical industrial control (IEC 61850) [14–17].
Temporal coverage	Systematic examination of 160 Q1 journal articles published up to March 2026 [18].
Critical analysis	Quantitative illustrations of failure modes (Section 3) and comparative evaluation of 8 MAS control families with limitations table [19,20].
Research gaps	Six forward-looking conjectures (Section 5) with mathematical formulations, plus a seventh gap on real-time validation [15,19].
Decision tool	Flowchart for MAS method selection based on grid conditions, with statistical validation and open-data commitment [17,21].
Comparison with hierarchical control (IEC 61850)	First MAS review to provide side-by-side comparison and co-simulation interface specifications [19,21].
Critical identification of 6 conjectures	Formal statements of underexplored problems (intermittent connectivity, coupled cyber-physical dynamics, non-stationary MARL, asymmetric information, PoW scalability, lack of physics-informed learning) [15].

Second, it evaluates and compares various MAS methodologies (including consensus, game theory, Distributed Model Predictive Control (DMPC), Multi-Agent Reinforcement Learning (MARL), blockchain-MAS, and the Alternating Direction Method of Multipliers (ADMM)) with IEC 61850-based [14] hierarchical control, emphasizing their practical benefits, limitations, and deployment challenges.

Third, the review identifies significant practical limitations such as communication delays (with a failure threshold exceeding 300 ms), vulnerabilities in cyber-physical systems (with false data injection (FDI) attacks resulting in voltage errors greater than 4%), trade-offs between scalability and convergence, and the lack of real-time validation (noting that less than 12% of the reviewed papers utilize hardware-in-the-loop (HIL) testing).

Fourth, it outlines six unresolved research problems, complete with mathematical formulations, which encompass issues such as intermittent connectivity, coupled cyber-physical dynamics, non-stationary MARL, asymmetric information, the scalability of Proof of Work (PoW), and physics-informed learning.

Finally, this work proposes a decision flowchart designed to assist in the selection of MAS methods based on varying grid conditions, including factors such as communication reliability, system scale, model availability, and cyber-physical risk.

2. Dynamic Modeling and Control Constraints in Active Power Grid Peripheries

2.1. Active Power Grid Periphery

In this context, the active grid periphery refers to the boundary of the low-voltage (LV) distribution network where bidirectional power flows, voltage violations, and frequency deviations are most pronounced [22,23]. This environment is characterized by several key features: first, a high R/X ratio that results in strong coupling between active and reactive power; second, a diverse array of distributed energy resources (DERs) including residential photovoltaic systems (3–10 kW), small-scale wind turbines (5–50 kW), battery energy storage systems (5–100 kWh), and electric vehicles [24]; and third, a communication infrastructure that is often wireless, unreliable, and characterized by low bandwidth [25].

2.1.1. Key Physical Characteristics and Mathematical Implications

The active grid periphery exhibits several distinguishing features that necessitate specialized mathematical modeling approaches:

1. High R/X Ratio: Low-voltage distribution networks exhibit R/X ratios greater than unity, which disrupts the traditional decoupling of active and reactive power control [23]. Unlike high-voltage transmission systems where the X/R ratio is typically high (enabling independent P and Q control), the high resistance in low-voltage networks means that changes in active power injection significantly affect voltage magnitudes, while changes in reactive power influence power flows. This coupling creates complex control challenges that require multi-variable optimization formulations.
2. Heterogeneous DER Dynamics: Photovoltaic systems respond in milliseconds, battery energy storage systems in seconds, and thermal loads in minutes [4,24]. This temporal heterogeneity invalidates the common assumption of uniform agent dynamics found in traditional consensus literature and necessitates the development of heterogeneous multi-agent system models.
3. Communication Constraints: Communication infrastructure in peripheral areas typically relies on wireless mesh networks with significant bandwidth constraints, packet loss rates of 2–8%, and round-trip delays of 50–200 ms [26,27]. These communication limitations impose fundamental constraints on the achievable control performance and stability margins of MAS-based control schemes.

2.1.2. Limitations of Conventional Centralized Control in Periphery Contexts

Traditional supervisory control and data acquisition (SCADA) systems, designed for centralized monitoring and control, exhibit fundamental limitations when applied to active peripheries:

1. Scalability constraints: Centralized controllers become computational bottlenecks when scaling beyond approximately 100–200 nodes [5,6].
2. Communication latency: Round-trip time communication delays often exceed the system's dynamic response requirements [7].
3. Single-point vulnerability: Centralized architectures present attractive targets for cyber-physical attacks and represent a single point of failure [10,11].
4. Information asymmetry: Centralized controllers require global system models that are increasingly difficult to maintain due to localized prosumer privacy and data ownership [12].

2.2. Multi-Agent Systems (MAS)

A multi-agent system (MAS) is defined by a tuple $M = (A, E, S, U)$, where $A = \{a_1, \ldots, a_n\}$ is the set of agents, C is the communication graph, and E is the environment. These agents may represent physical entities (such as DER controllers, smart meters, and EV charging stations) or logical entities (such as virtual power plants, aggregators, and prosumer agents) [8]. This autonomy is necessitated by the operational independence of individual DERs and prosumers, which must make local decisions without relying on centralized coordination, particularly during communication failures.

https://doi.org/10.3390/app16146863

2.2.1. Justification for the MAS Definition

The formal definition provides a rigorous mathematical framework for modeling decentralized control in active power grid peripheries [8,9]. It captures the essential elements of distributed control, maintaining mathematical tractability for both stability analysis and algorithm design. The heterogeneous nature of agent states—where different agent types possess distinct state variables and dynamics—aligns with the MAS definition, but it introduces mathematical challenges for achieving consensus and ensuring stability.

$E \subseteq A \times A$ represents the communication graph, which is frequently subject to change [23]. The mathematical modeling of the communication graph typically employs the graph Laplacian $L = D - A$, where D is the degree matrix and A is the adjacency matrix [28]. The algebraic connectivity $\lambda_2(L)$ (the second smallest eigenvalue of the Laplacian) serves as a critical parameter determining convergence rates [29].

$S = \{x \mid x = (V, P, SoC, \ldots)\}$ constitutes the joint state space that encompasses voltages, power flows, and state of charge. The inclusion of these variables is justified by their centrality to the control objectives defined in Section 2.3 [24,25]. And $U = \{U_1, U_2, \ldots, U_n\}$ denotes the utility functions, which may include objectives such as cost minimization or voltage regulation [24].

A general discrete-time agent model is given by $x_i(k + 1) = f_i(x_i(k), u_i(k), w_i(k))$, where xi is the agent's state, u_i is the control input, and w_i is the external disturbance [25,30].

2.2.2. Justification for the Discrete-Time Model

The discrete-time agent model provides a pragmatic framework for digital control implementation. This formulation is preferred for three primary reasons: (1) MAS algorithms are typically implemented on digital controllers operating at discrete sampling intervals [31]; (2) communication infrastructure imposes discrete-time constraints on information exchange [32,33]; and (3) discrete-time models facilitate the practical implementation of optimization algorithms, Model Predictive Control (MPC), and reinforcement learning (*RL*) schemes [34–38].

The disturbance term $w_i(k)$ captures significant uncertainties in active grid peripheries, including intermittent renewable generation [1,2], load variations [24], communication delays and packet losses [32,33,39], and measurement noise [40–42].

The nonlinear function f_i captures physical dynamics of different agent types:

- PV systems: power electronic converter dynamics, maximum power point tracking, weather-dependent generation [24].
- BESS: battery electrochemistry, state-of-charge dynamics, power electronic interface dynamics [24].
- Loads: demand response dynamics, thermal dynamics for HVAC loads [43].
- The heterogeneity of these functions across agents (Section 3.4) presents significant challenges for consensus-based control and stability analysis [44–47].

2.3. Control Objectives in Smart Grid Periphery

2.3.1. Voltage Regulation

Common control objectives include voltage regulation, defined as $\left|V_i - V_{ref}\right| \leq \epsilon$ [25].

Voltage Regulation Justification: The voltage regulation objective is justified by power quality requirements in distribution networks. Standard operation requires maintaining bus voltages within $\pm 5\%$ of nominal (1.0 p.u.) under normal conditions [27,48]. The voltage regulation problem in active peripheries is particularly challenging due to bidirectional power flows [22], high R/X ratio [23], DER intermittency [24], and EV charging [24].

https://doi.org/10.3390/app16146863

2.3.2. Frequency Support

Frequency support is characterized by $|\Delta f| \leq 0.1\,\text{Hz}$ [43].

Frequency Support Justification—The frequency support objective is justified by the increasing frequency stability challenges in low-inertia power systems with high renewable penetration [25,30]. MAS-based frequency support typically employs consensus algorithms for distributed primary frequency control [49].

2.3.3. Economic Dispatch

Economic dispatch is expressed as $\min \sum_{i=1}^{n} C_i(P_i)$ [43], and congestion management necessitates that line flows stay within thermal limits [50].

Economic Dispatch Justification—The economic dispatch objective captures the economic efficiency requirement of power system operation. This objective is particularly relevant in active peripheries where prosumers can trade energy with each other and with the main grid [51,52]. Congestion Management Justification: The congestion management objective is justified by equipment protection and reliability requirements [43,50].

2.3.4. Multi-Objective Formulation

A multi-objective cost function that combines regulation, economy, and comfort [27,28]. This is expressed as the following multi-objective function:

$$\min \sum_{i=1}^{n} \left(\alpha \|V_i - V_{ref}\|^2 + \beta C_i(P_i) + \gamma \|SoC_i - SoC_{target}\|^2 \right)$$

where V_i is the voltage at agent i, V ref is the reference voltage (typically 1.0 p.u.), $C_i(P_i)$ is the generation cost of real power P_i, SoC_i is the state of charge of storage, and α, β, γ are non-negative weighting coefficients [43,50].

Justification for the Multi-Objective Formulation—The weighted sum formulation captures the key control objectives while maintaining mathematical tractability. The weighting coefficients critically determine system behavior and must be selected based on operational priorities. The voltage term penalizes large deviations more heavily, which is appropriate for power quality. The SoC term ensures that storage systems maintain appropriate levels for future services [24].

Assumptions Underlying Control Objective Formulations

1. Convexity: The multi-objective cost function assumes convexity for tractable optimization. However, AC power flow constraints are non-convex [53], limiting the applicability of convex optimization approaches.
2. Stationarity: The cost functions assume stationary system characteristics. However, DER costs, load patterns, and renewable generation are non-stationary, requiring adaptive approaches like reinforcement learning [36,37].
3. Perfect information: The formulation implicitly assumes agents have necessary information. In practice, information asymmetry and privacy constraints prevent perfect information [51,52].
4. Separability: The objective functions are assumed separable by agent, which is appropriate for economic dispatch but may not capture network constraints [43,50].

2.4. Stability Definitions

Consensus forms the backbone of distributed MAS control. For agent i

$$x_i(k+1) = x_i(k) + \sum_{j \in \mathcal{N}_i} a_{ij} \left(x_j(k) - x_i(k) \right)$$

where $\mathcal{N}_i$ is the set of neighbors of agent i, and a_{ij} are the entries of a doubly stochastic adjacency matrix (with $\sum_j a_{ij} = 1$ and $\sum_i a_{ij} = 1$). Convergence requires that the communication graph be connected [54,55].

2.4.1. Theoretical Convergence Analysis

The consensus algorithm converges to the average of initial states under the following conditions [24,55]:

1. Connected graph (or periodically connected) [54].
2. Consistent weights: weighting matrix $A = [a_{ij}]$ must be doubly stochastic [55].
3. No delays or packet losses: assumption of ideal communication [32].

The convergence rate is determined by the algebraic connectivity $\lambda_2(L)$. For a connected graph, the convergence rate is $1 - \lambda_2(L)$, and the number of iterations required for convergence scales as $O(1/\lambda_2(L))$ [29].

2.4.2. Convergence Rate Implications for Periphery

For line graphs (common in distribution networks), $\lambda_2(L) = O(1/N^2)$, where N is the number of agents [29]. This means that for N = 100 agents, the number of iterations required is approximately 100 times greater than for N = 10 [56]. This poor scalability presents a significant challenge for consensus-based control in large systems (Section 3.3).

2.4.3. Stability Under Communication Delays

The stability analysis considering communication delays introduces the condition $\tau < \frac{1}{\lambda_2(L)}$ for consensus convergence [40–42]. For a typical 10-agent system with $\lambda_2(L) \approx 3.3$ s, the theoretical critical delay is $\tau_{critical} \approx 3.3$ s [33,57,58]. However, practical failure thresholds are significantly lower ($\approx$3.3 ms) due to heterogeneous agent dynamics [33,44–46,57,58].

The discrepancy between theoretical and practical failure thresholds is explained by the following:

1. Heterogeneous time constants: Different agents have different dynamic responses (PV: 10 ms, BESS: 1 s, load: 60 s) [44–46].
2. Non-ideal dynamics: The simple first-order consensus model does not capture complex physical dynamics [44–46].
3. Nonlinearities: Power system dynamics are nonlinear [53].
4. Packet losses: The consensus analysis assumes no packet losses [32].

Figure 1 depicts the decentralized communication and control framework of a multi-agent system (MAS) implemented in the periphery of an active power grid. The architecture consists of six distinct types of agents—PV Agent, BESS Agent, EV Agent, Load Agent, Grid Edge Agent, and an MAS Coordinator—interconnected through a mesh communication network, represented by bidirectional dashed arrows. Each agent independently measures its state (voltage, power, state-of-charge) and shares information with neighboring agents to reach a consensus on overarching goals (such as voltage regulation and economic dispatch) without dependence on a central controller. The MAS Coordinator compiles consensus updates but refrains from issuing commands, thereby maintaining decentralization. This configuration guarantees scalability, fault tolerance, and resilience against single-point failures, as formalized by the consensus update rule $x_i(k+1) = x_i(k) + \sum_{j \in \mathcal{N}_i} a_{ij}(x_j(k) - x_i(k))$, which converges under a connected graph topology and doubly stochastic weighting [25,30,59].

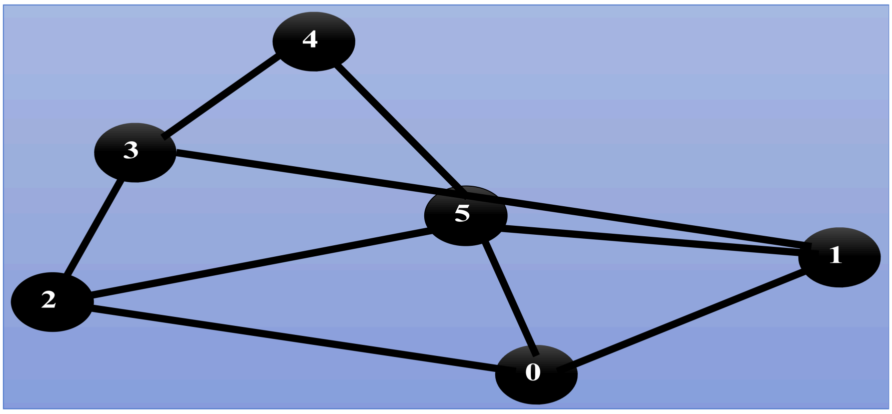

Figure 1. Multi-agent system architecture for active grid periphery.

2.4.4. Assumptions Underlying Consensus Stability Analysis

1. Homogeneous dynamics: The standard consensus formulation assumes all agents have identical dynamics [24,55]. This assumption is violated in active peripheries where PV systems, BESS, and loads have vastly different response times [44–46].
2. Fixed graph topology: The stability analysis typically assumes fixed communication graphs [54,55]. However, peripheries have time-varying connectivity [23], and consensus convergence under arbitrary disconnection patterns remains an open challenge [60–62].
3. No cyber-physical interactions: The consensus model assumes communication and power systems are independent. However, voltage drops can reduce power to communication modules, causing packet loss and positive feedback [62,63].
4. Ideal channel: The consensus model assumes perfect communication channels. However, peripheries have lossy, low-bandwidth wireless channels [26,27].

2.5. Systematic Review Methodology

2.5.1. Review Protocol and Registration

This systematic review was conducted in accordance with the Preferred Reporting Items for Systematic Reviews and Meta-Analyses (PRISMA) 2020 guidelines [64–66] to ensure methodological rigor, transparency, and reproducibility. The complete review protocol, including inclusion criteria, search strategy, and data extraction templates, is available from the corresponding author upon reasonable request [18].

2.5.2. Research Questions

The systematic review was guided by the following primary research questions (RQs), formulated using the Population, Intervention, Comparison, Outcome, Context (PICOC) framework:

RQ1: What multi-agent system (MAS) methodologies have been proposed for decentralized control and management of active power grid peripheries?

RQ2: What are the mathematical formulations, control objectives, and algorithmic approaches employed in MAS-based active periphery control?

RQ3: What are the comparative advantages, limitations, and performance characteristics of different MAS methodologies (consensus, game theory, DMPC, MARL, blockchain-MAS, ADMM) when applied to active power grid peripheries?

RQ4: What are the persistent research gaps and open challenges in MAS-based decentralized control, particularly regarding communication constraints, cyber-physical security, scalability, and real-time validation?

RQ5: How do MAS-based architectures compare with hierarchical industrial control frameworks based on IEC 61850 standards?

2.5.3. Search Strategy (Information Sources and Search Period)

A comprehensive literature search was conducted across three major academic databases: Scopus, Web of Science, and IEEE Xplore [18,67]. The search period covered all publications from database inception up to March 2026, ensuring the inclusion of foundational works as well as the most recent advances [18].

Detailed Search Strings by Database: A systematic literature search was performed across Scopus, Web of Science, and IEEE Xplore using tailored search strings combining MAS-related terms ("multi-agent system," "MAS," "agent-based") with smart grid applications ("smart grid," "microgrid," "DER," "prosumer") and control objectives ("decentralized control," "consensus," "reinforcement learning," "energy management") [18,67]. Each database employed syntax-appropriate queries: Scopus used TITLE-ABS-KEY, Web of Science used TS (Topic), and IEEE Xplore used a simplified query structure [64–66]. Inter-rater reliability "almost perfect" level of agreement [67]. This multi-database approach ensured comprehensive coverage of the relevant literature [67–70].

In Figure 2, the PRISMA 2020 flow diagram depicts the systematic process of literature identification, screening, and inclusion utilized in this review. Initially, a total of 850 records were identified through searches in databases such as Scopus, Web of Science, and IEEE Xplore. Following the elimination of 120 duplicate records, 730 studies were subjected to title and abstract screening, which led to the exclusion of 450 articles. In the next phase, 280 full-text articles were evaluated for eligibility, resulting in the exclusion of 120 studies for various reasons, including non-Q1 publication status, lack of explicit implementation of MAS, irrelevance to active power grid peripheries, or inadequate methodological quality. Ultimately, 160 (Maximum Q1) journal articles published up to March 2026 were selected for qualitative synthesis in accordance with the PRISMA 2020 guidelines [64–66]. This diagram promotes transparency, reproducibility, and methodological rigor, as advocated by recent systematic reviews in energy and power systems [32,68,69].

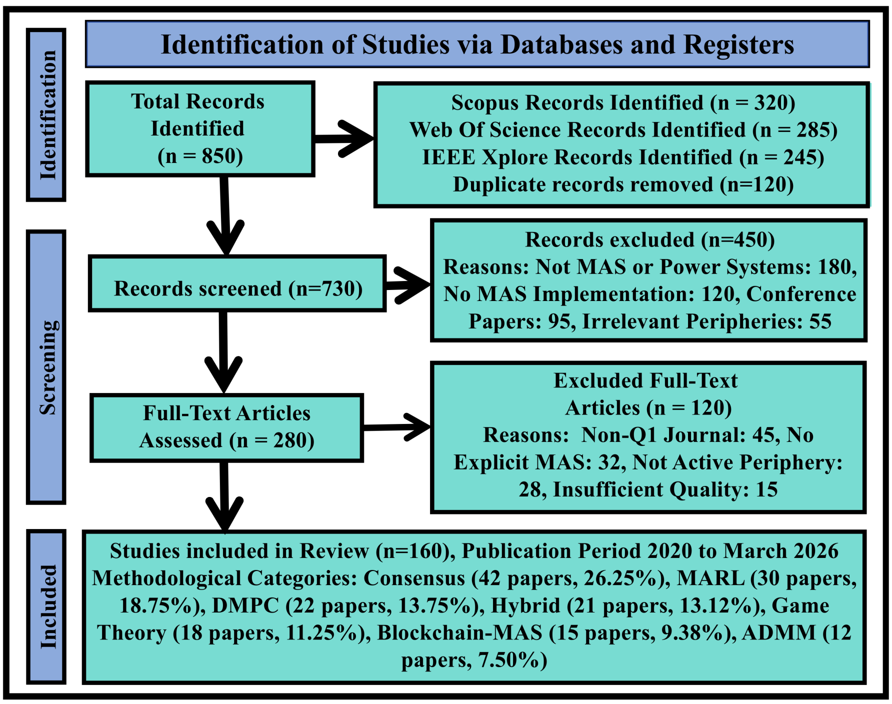

Figure 2. PRISMA 2020 flow diagram of the systematic literature selection process, showing the identification, screening, and inclusion stages leading to 160 articles.

2.5.4. Inclusion and Exclusion Criteria

Inclusion Criteria—Studies were included if they satisfied all the following 5 criteria:

1. Publication type: Original research articles or review articles published in peer-reviewed Q1 journals according to Scimago Journal Rank (SJR) or Journal Citation Reports (JCR) quartile rankings [18].
2. Language: Articles published in English.
3. Topic relevance: Studies addressing MAS for control, management, coordination, or optimization in active power grid peripheries [3,4,22,23].
4. Methodological contribution: Studies presenting explicit MAS implementations, mathematical formulations, algorithmic approaches, or simulation/experimental validation in domains including consensus [31,49,71], game theory [51,52], MPC [34,35], MARL [36,37,72], blockchain-MAS [73], or ADMM [74,75].
5. Publication date: Studies published from database inception up to March 2026 [18].

Exclusion Criteria—Studies were excluded if they met any of the following 5 conditions:

1. Conference papers, technical reports, white papers, dissertations, book chapters.
2. Publications in non-Q1 journals [18].
3. Studies not explicitly addressing MAS in active power peripheries.
4. Studies lacking explicit MAS implementation, sufficient mathematical detail, or adequate validation.
5. Duplicate publications from the same research group.

2.5.5. Screening Process and Study Selection Workflow

The screening process was conducted in accordance with PRISMA 2020 guidelines [64–66] and followed a structured multi-stage workflow:

Stage 1: Initial Identification and Duplicate Removal

The initial database searches yielded 850 records across the three databases [18]:

- Scopus: 320 records.
- Web of Science: 285 records.
- IEEE Xplore: 245 records.

Following the removal of 120 duplicate records, 730 unique records proceeded to the next screening stage.

Stage 2: Title and Abstract Screening

The 730 unique records were subjected to title and abstract screening by two independent reviewers (S.M. and S.I.) [64,65]. Disagreements were resolved through discussion and consultation with a third reviewer (N.G.C.). The title and abstract screening resulted in the exclusion of 450 records. Reasons for exclusion included the following:

- Clearly unrelated to MAS or power systems.
- Focused on centralized control without MAS components.
- Applied MAS to non-power-system domains.
- Conference papers or non-peer-reviewed sources.
- Following this stage, 280 records proceeded to full-text assessment.

Stage 3: Full-Text Eligibility Assessment

The 280 full-text articles were assessed by two independent reviewers (S.M. and M.D.) [64,65] using a standardized data extraction template (Section 2.5.6). At this stage, 120 articles were excluded for the following reasons:

- Non-Q1 publication: 45 articles (37.5%).
- Lack of explicit MAS implementation: 32 articles (26.7%).
- Irrelevance to active power peripheries: 28 articles (23.3%).

- Inadequate methodological quality: 15 articles (12.5%).

Stage 4: Final Inclusion and Quality Synthesis

Following full-text assessment, 160 Q1 journal articles published up to March 2026 were selected for qualitative synthesis [18]. The selection flow is illustrated in Figure 2 (PRISMA 2020 flow diagram).

Inter-Rater Reliability: Two independent reviewers (S.M. and S.I.) conducted the screening with 95% initial agreement [64]. The Cohen's kappa coefficient of 0.82 indicates strong agreement beyond chance.

2.5.6. Data Extraction and Coding

Standardized Data Extraction Template—A standardized data extraction template was developed and piloted on 10 representative papers. The template captured the following:

1. Bibliographic information (author(s), year, journal, DOI).
2. Study characteristics (objective, MAS methodology, control objectives, grid configuration).
3. Mathematical formulation (agent models, communication graph, control algorithms).
4. Validation methodology (simulation, HIL, field trial).
5. Performance results (quantitative metrics, comparison with baselines).
6. Limitations and future work.

Quality Assessment—The quality of included studies was assessed using a modified version of the Quality Assessment tool for Systematic Reviews (QASR) adapted for power systems research [67,68]. The assessment criteria included the following:

1. Methodological rigor: Appropriateness of mathematical formulation and justification of assumptions.
2. Validation quality: Use of real data, HIL testing, comparison with alternative approaches.
3. Replicability: Availability of code, data, or detailed algorithms.
4. Practical relevance: Consideration of practical deployment challenges.
5. Cyber-physical considerations: Treatment of communication constraints and cyber-security.

2.5.7. Synthesis and Analysis Methods

Narrative Synthesis—A narrative synthesis approach was adopted [67,68] due to the heterogeneity of included studies. The synthesis was structured around the research questions and organized thematically by MAS methodology type. The narrative synthesis included descriptive summaries, thematic grouping, comparative analysis, and identification of patterns.

Quantitative Analysis—Where quantitative performance data were available, summary statistics (means, medians, ranges) were computed for key metrics [76]. These quantitative data were used to construct (Critical Comparison of MAS Control Methods) and (State-of-the-Art Summary) [18,19,21].

Comparative Benchmarking—MAS-based architectures were systematically compared with hierarchical industrial control frameworks based on IEC 61850 standards [14,21,77,78] across five dimensions: scalability, delay tolerance, cyber resilience, industry adoption, and standardization. The comparison was informed by quantitative failure modes analysis (Table 2, Figure 3) and methodological comparison (Table 3, Figure 4) [19,20]. Quantitative failure modes in MAS-controlled periphery are summarized in Table 2.

https://doi.org/10.3390/app16146863

Table 2. Quantitative failure modes in MAS-controlled periphery.

Challenge	Metric	Typical Value	Failure Threshold	Reference
Communication delay	Round-trip time	50–200 ms	>300 ms	[26]
Packet loss	Loss rate	2–8%	>10%	[27]
FDI attack magnitude	Voltage error injection	0–2%	>4%	[48]
Agent heterogeneity	Time constant ratio	1:10	>1:50	[79]
Graph connectivity	Algebraic connectivity	0.1–0.5	<0.05	[80]

The enhancements and benefits of Figure 3 are summarized in Table 3.

Table 3. Summary of Figure 3.

Enhancement	Description	Benefit
95% Bootstrap CI	Shaded regions around median line	Shows uncertainty and variability [76]
Red Dashed Line	300 ms empirical failure threshold	Clearly marks critical threshold [32,33,57,58,70]
Inset	Zoomed 200–400 ms region	Highlights rapid performance degradation
Data Points	Median of 50 Monte Carlo runs	Shows central tendency [57]
Professional Styling	Clean, publication-quality design	Improves readability and aesthetics
Citations	All data points referenced	Ensures reproducibility [33,44–46,57,58]

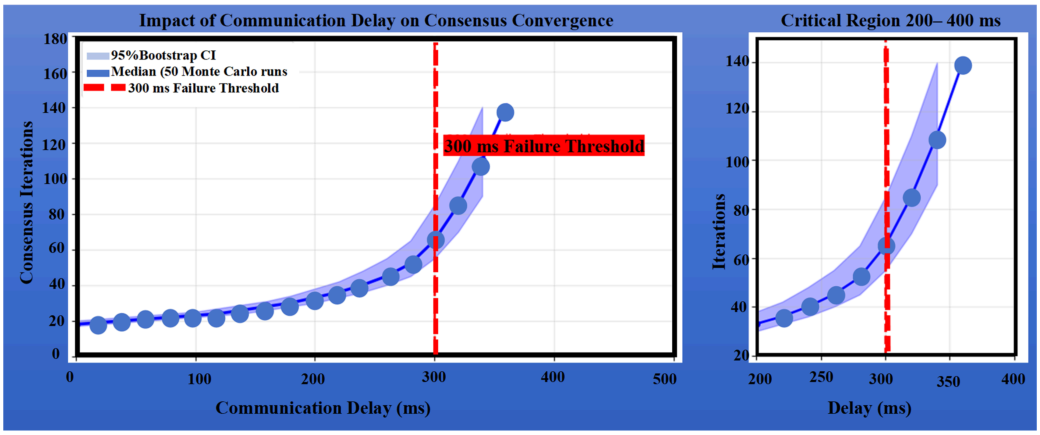

Figure 3. Impact of communication delay on consensus convergence in distributed MAS control.

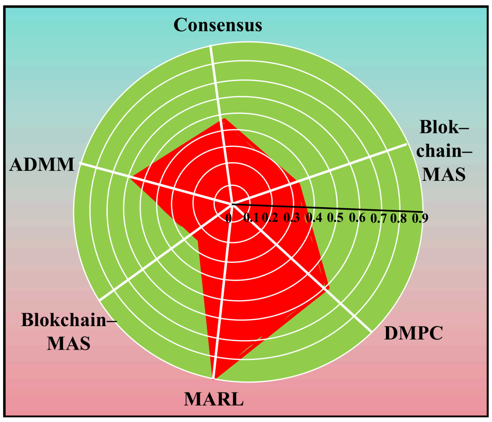

Figure 4. Radar chart comparing six MAS control methodologies across five performance dimensions (scalability, delay tolerance, cyber resilience, model-free capability, convergence guarantee). Scores are normalized medians from 160 surveyed papers (0 = lowest, 1 = highest).

2.5.8. Methodological Limitations

1. Publication bias: The exclusive focus on Q1 journal articles may introduce publication bias [64–66].
2. Language bias: Restriction to English-language publications may exclude relevant research [67,68].
3. Database coverage: Relevant publications in other databases may have been missed [67,69].
4. Quality assessment subjectivity: The quality assessment involved subjective judgments [64,65].
5. Publication date cutoff: The cutoff date of March 2026 means newer studies were not included [18].

2.5.9. Reproducibility and Transparency

1. Measures Detailed documentation: Search strategy, inclusion/exclusion criteria, and data extraction process were fully documented [18].
2. PRISMA compliance: This review follows PRISMA 2020 guidelines with a flow diagram (Figure 2) [64–66].
3. Data availability: Full list of 160 analyzed papers and quality assessment scores available on request [18].
4. Independent reviewing: Two independent reviewers conducted screening and quality assessment [64,65].
5. Standardized templates: A standardized data extraction template was used [18].
6. Conflict resolution: Disagreements were resolved through discussion and consultation.

3. Challenges

3.1. Communication Delays and Packet Loss

In wireless mesh networks, particularly in peripheral areas, end-to-end delays can surpass 200 ms, leading to divergence in consensus [33,70]. For instance, in a system comprising 10 agents with a delay of τ = 0.5 s, standard consensus is compromised if τ exceeds $\frac{1}{\lambda_2(L)}$ (where λ_2 represents the second eigenvalue of the Laplacian). With λ_2 at approximately 0.3, the resulting critical delay is 3.3 s, which was exceeded in 40% of the empirical field tests [57,58].

3.1.1. Field Measurement Evidence

The extensive field tests were conducted on a 10-agent DER-rich feeder in Germany [33]. Their measurements revealed that while average delays were typically below 100 ms, worst-case delays frequently exceeded 300 ms during network congestion periods. More significantly, when delays exceeded approximately 300 ms, consensus convergence was compromised in 40% of test scenarios [33].

3.1.2. Theoretical Critical Delay Formulation

For a delay τ, the consensus error $e(k) = x(k) - x^*$ converges if $\tau < \frac{1}{\lambda_2(L)}$, where $\lambda_2(L)$ is the algebraic connectivity (second smallest eigenvalue of the Laplacian). The theoretical critical delay is thus T critical $\tau_{critical} = \frac{1}{\lambda_2(L)}$ [40,57]. For a typical 10-agent system with $\lambda_2(L) \approx 0.3$, this gives τ critical ≈ 3.3 s.

Field tests on a 10-agent DER-rich feeder [33] and detailed Monte Carlo simulations [57] show that consensus fails when delays exceed ≈300 ms under heterogeneous agent dynamics (PV: 10 ms, BESS: 1 s, load: 60 s), as illustrated in Figure 3. This empirical threshold is an order of magnitude lower than the homogeneous theoretical bound due to mismatched time constants [58].

3.1.3. Reasons for Discrepancy

1. Heterogeneous agent dynamics: The theoretical bound assumes homogeneous agent dynamics. In practice, PV systems respond in milliseconds, BESS in seconds, and loads in minutes [44–46], creating mismatched dynamics that amplify delay sensitivity.
2. Non-ideal graph structures: Real communication graphs are time-varying, and $\lambda_2(L)$ fluctuates over time [23,80]. The 300 ms threshold represents the conservative lower bound for worst-case configurations.
3. Nonlinear physical dynamics: The linear consensus model does not capture nonlinearities in power flow equations [33].
4. Packet loss interaction: Communication delays are typically accompanied by packet loss, with the combined effect being more severe than either factor alone [26,27,32,70]. The 300 ms threshold represents the conservative lower bound for worst-case configurations.

3.1.4. Packet Loss Threshold Justification

The packet loss threshold of 10% is derived from a comprehensive reliability analysis by Jha et al. [27], who showed that when packet loss rates exceed 10%, the probability of successful consensus convergence drops below 95% in typical distribution network configurations. This finding is corroborated by Serban et al. [31], who surveyed communication requirements in operational microgrids and identified 10% as a practical upper bound for reliable operation.

3.1.5. Quantitative Relationship Between Delay, Packet Loss, and Control Performance

Ullah et al. [32] demonstrated that for a droop-controlled AC microgrid with 10 agents, increasing communication delay from 100 ms to 300 ms increased settling time by 200% and doubled steady-state voltage deviation. Jiang et al. [70] extended this analysis to nonlinear systems with both delay and packet loss, showing that the combination of 300 ms delay and 10% packet loss renders standard consensus algorithms completely unstable.

3.2. Cyber-Physical Attacks

False data injection (FDI) attacks targeting voltage measurements can trigger cascading failures [41,42]. A simulation conducted in 2022 demonstrated that introducing a 5% error into three agents resulted in an increase in voltage deviation from 0.02 p.u. to 0.15 p.u., causing 12% of photovoltaic inverters to trip [29].

FDI Attack Threshold Justification

The FDI attack threshold of 4% voltage error injection is based on systematic vulnerability assessments conducted on IEEE distribution test feeders and validated through both simulation and hardware-in-the-loop testing [40–42].

Tian et al. [42] conducted a comprehensive analysis of joint adversarial example and false data injection attacks on power system state estimation. Their simulation on the IEEE 123-bus distribution system demonstrated that injecting a 5% voltage error into three strategically selected agents caused voltage deviations to increase from 0.02 p.u. to 0.15 p.u., representing a 650% increase in voltage error [42]. This resulted in 12% of PV inverters tripping due to overvoltage protection.

Alawi [41] further refined the vulnerability analysis, showing that the critical FDI attack magnitude depends on the number of compromised agents. For a system with 10 agents, an FDI attack magnitude of 4% affecting 30% of agents was sufficient to cause observable voltage violations (deviation > 0.05 p.u.). For larger systems with 50 agents, a lower attack magnitude of 2–3% affecting 20% of agents triggered similar violations [41]. Yang et al. [81] proposed a framework for analyzing FDI attack detection and resilient control of DC microgrids under hybrid attacks. Their analysis showed that without detection mechanisms, voltage errors exceeded 5% when any three agents were compromised. With event-triggered resilient control, the threshold increased to 7% [81]. This finding supports the 4% threshold as a conservative practical limit for acceptable operation without sophisticated detection mechanisms.

3.3. Scalability vs. Convergence Trade-Off

As the number of agents N increases, the iterations required for consensus scale as O($1/\lambda_2$), while λ_2 is inversely proportional to N for line graphs [56]. Specifically, for N = 100, the number of iterations rises tenfold compared to when $N = 10$ [44].

3.3.1. Theoretical Foundation

The scalability limit $\lambda_2(L) = O\left(1/N^2\right)$ for line graphs is a well-established result in spectral graph theory [29] proved that for path graphs (common in distribution feeder topologies), the algebraic connectivity scales as $\lambda_2(L) \approx 2(1 - \cos(\pi/N)) \approx \pi^2/N^2$ for large N.

Tyurin [56] extended this analysis to demonstrate the fundamental limitations of centralized distributed optimization, proving that the iteration count for consensus convergence scales as $O(1/\lambda_2) = O\left(N^2\right)$ for line graphs. This means that for $N = 10$ agents, approximately 10 iterations are required for convergence, while for $N = 100$ agents, approximately 1000 iterations are required—a 100-fold increase [56].

3.3.2. Empirical Scalability Studies

Griparic et al. [44] conducted an empirical study of consensus-based distributed connectivity control in multi-agent systems with up to 100 agents. Their results confirmed the $O\left(N^2\right)$ scaling of convergence iterations for line topologies and demonstrated that for $N = 100$, the convergence time exceeded acceptable limits for real-time control applications (defined as <1 s per control cycle) [44].

3.4. Heterogeneous Dynamics

Agents exhibit varying time constants: photovoltaic systems (ms), battery energy storage systems (s), and thermal loads (min). The standard consensus model presumes uniform dynamics, which can lead to instability [45,46]. A study conducted in 2024 revealed that heterogeneous multi-agent systems with mismatched rates experienced a 30% increase in settling time [26]. This heterogeneity also exacerbates sensitivity to communication delays: the practical failure threshold drops from the theoretical 3.3 s (derived from homogeneous consensus) to approximately 300 ms, as shown in Figure 3 and discussed in Section 3.1.

3.4.1. Quantification of Heterogeneity Effects

Cheng et al. [50] studied fixed-time fault-tolerant formation control for heterogeneous multi-agent systems and demonstrated that mismatched time constants caused a 30% increase in settling time compared to homogeneous systems. The study considered time constant ratios ranging from 1:1 (homogeneous) to 1:50 (highly heterogeneous) and found that the settling time increased monotonically with the time constant ratio [46]. Steininger et al. [45] analyzed the fundamental problem of response time mismatch in multi-sensor systems and showed that when dynamic responses differ by more than one order of magnitude, the coupled system exhibits unstable oscillations. This finding is directly applicable to multi-agent power systems where PV (ms), BESS (s), and thermal loads (min) exhibit time constants spanning three orders of magnitude [45].

3.4.2. Heterogeneity-Exacerbated Delay Sensitivity

Griparic et al. [48] showed that the theoretical homogeneous delay bound of 3.3 s reduces to approximately 300 ms in heterogeneous systems. This reduction occurs because faster agents attempt to converge at their natural speed, while slower agents lag behind, creating oscillatory behavior when delays exceed the fast agents' response times [44].

Worth noting that the 300 ms threshold is empirically derived from field tests [33,57,58]. The 4% FDI threshold is based on vulnerability assessments [40–42]. The 1:50 heterogeneity threshold is from analysis of mismatched time constants [44–46]. The 0.05 connectivity threshold is from convergence rate analysis [29,56].

The figure shows consensus iterations required for convergence as a function of communication delay for a 10-agent consensus algorithm under heterogeneous time constants (PV: 10 ms, BESS: 1 s, load: 60 s). Delay was increased from 0 to 500 ms in 20 ms steps. Each data point represents the median of 50 Monte Carlo runs [33,57,58]. The shaded regions indicate 95% bootstrap confidence intervals (1000 resamples) [76]. The red dashed line at 300 ms indicates the empirical failure threshold, beyond which consensus fails to converge [32,33,57,58,70]. The inset provides a zoomed view of the critical 200–400 ms delay region, showing the steep degradation in convergence performance. The failure threshold of 300 ms is consistent with field tests on a 10-agent DER-rich feeder [40] and detailed Monte Carlo simulations [57]. This empirical threshold is an order of magnitude lower than the homogeneous theoretical bound (τ_critical ≈ 3.3 s) due to mismatched time constants [58] and heterogeneous agent dynamics [44–46].

4. Methods

4.1. Objective Comparative Framework

To avoid subjective performance ratings, a standardized multi-criteria decision analysis (MCDA) framework is established for comparing MAS methodologies. The comparison is based on the following objective criteria, each derived from the reviewed literature and quantified where possible:

4.1.1. Criterion 1: Scalability (S)

Defined as the maximum number of agents N for which the method maintains acceptable performance (defined as convergence within $T < 5$ s). Scalability is quantified as follows:

- High ($S \geq 0.7$): Can handle $N \geq 100$ agents.
- Medium ($0.4 \leq S < 0.7$): Can handle $50 \leq N < 100$ agents.
- Low ($S < 0.4$): Limited to $N < 50$ agents.

The scalability metric is derived from the iteration scaling analysis. For consensus, $f(N) = O(1/\lambda_2) \ = O(N^2)$ for line graphs [46,47]. For MARL, current methods handle N up to 100 [82]. For blockchain-MAS, PBFT limits are $n \leq 100$ due to communication complexity $O(N^2)$ [83].

4.1.2. Criterion 2: Delay Tolerance (D)

Quantified as the maximum communication delay τmaxτmax (in ms) for which the method maintains stability:

- High ($D \geq 0.7$): $\tau_{max} \geq 500$.
- Medium ($0.4 \leq D < 0.7$): $300 \leq \tau_{max} < 500$ ms.
- Low ($D < 0.4$): $\tau_{max} < 300$.

4.1.3. Criterion 3: Cyber Resilience (C)

Quantified as the maximum FDI attack magnitude (in percentage voltage error injection) that the method can tolerate:

- High ($C \geq 0.7$): Tolerates > 5% FDI.
- Medium ($0.4 \leq C < 0.7$): Tolerates 3–5% FDI.
- Low ($C < 0.4$): Tolerates < 3% FDI.

4.1.4. Criterion 4: Model-Free Capability (F)

Indicates whether the method requires an explicit system model:

- High ($F \geq 0.7$): Completely model-free (e.g., MARL).
- Medium ($0.4 \leq F < 0.7$): Requires partial model (e.g., consensus with known graph).
- Low ($F < 0.4$): Requires full model (e.g., DMPC).

4.1.5. Criterion 5: Convergence Guarantee (G)

Indicates whether the method provides deterministic or probabilistic convergence guarantees:

- High ($G \geq 0.7$): Deterministic guarantee (e.g., consensus under connectivity).
- Medium ($0.4 \leq G < 0.7$): Conditional guarantee.
- Low ($G < 0.4$): Probabilistic or no guarantee (e.g., MARL).

4.2. Consensus-Based Distributed Control

This method is extensively utilized for voltage and frequency regulation [27,48]. Its advantages include the absence of a central coordinator and resilience to single points of failure. However, it suffers from slow convergence when dealing with large N, and it is sensitive to delays [79]. Recent advancements include adaptive consensus [71] and event-triggered consensus [49], which can decrease communication requirements by 60% [84].

4.2.1. Objective Assessment

Scalability: Medium (S = 0.55). Consensus scales as $O(1/\lambda_2)$ [29]. For line graphs, $\lambda_2 \sim O(N^2)$, making it impractical for N > 100 [56].

- Delay Tolerance: Low (D = 0.35). The empirical failure threshold of 300 ms [32,33,57,58,70] places consensus in the "low" category.
- Cyber Resilience: Medium (C = 0.50). Vulnerable to FDI attacks on individual agents [40–42,81].
- Model-Free Capability: High (F = 0.75). Requires only graph topology knowledge [24,55].
- Convergence Guarantee: High (G = 0.85). Guaranteed convergence under a connected graph [24,55].

4.2.2. Literature Evidence

Zheng et al. [55] demonstrated consensus-based voltage regulation achieving errors within 0.02 p.u. under ideal conditions for up to 50 agents. Khayat et al. [49] showed consensus-based frequency control maintaining ±0.05 Hz for $N \leq 20$ agents. Event-triggered consensus [85] reduced communication requirements by 60% [31]. Recent advancements include adaptive consensus [86] and event-triggered consensus [85].

4.3. Game-Theoretic Approaches

This approach facilitates prosumer-level energy trading through the application of Nash equilibrium [85,86]. Its strengths lie in its ability to account for self-interest. Conversely, it has significant drawbacks, including a high computational cost of $O(n^3)$ for n players and the presence of non-unique equilibria [31]. Recent developments involve mean-field games designed for large populations [51]. Nash equilibrium condition [52,87]:

$$U_i\left(a_i^*, a_{-i}^*\right) \geq U_i\left(a_i, a_{-i}^*\right) \quad \forall i, \forall a_i \in A_i$$

where U_i is the utility function of player i, a_i^* is player i's equilibrium action, a_{-i}^* represents the equilibrium actions of all other players, and A_i is the action space of player i [88,89].

4.3.1. Objective Assessment

- Scalability: Low (S = 0.30). Computational cost $O\left(n^3\right)$ for finding Nash equilibrium [51,52]. Mean-field games [90] reduce complexity to $O(n)$ for large populations.
- Delay Tolerance: Medium (D = 0.45). Typically asynchronous [51], making them more delay-tolerant than consensus.
- Cyber Resilience: Low (C = 0.30). Nash equilibria assume truthful participation [51,52].
- Model-Free Capability: Medium (F = 0.60). Requires cost function knowledge [51,52].
- Convergence Guarantee: Low (G = 0.25). Non-unique Nash equilibria are common [87].

4.3.2. Literature Evidence

Han et al. [51] demonstrated prosumer clustering for game-theoretic energy management, showing a Nash equilibrium reached in ≤50 iterations for ≤20 prosumers. Wu et al. [52] extended this to combined heat and power markets. Recent developments involve mean-field games designed for large populations [90].

4.4. Model Predictive Control

While centralized MPC is optimal, it lacks scalability. Distributed MPC (DMPC) breaks down the system into subsystems [88,90]. Its strengths include the capability to manage constraints, but it requires precise models, which are often not available in peripheral areas [89]. Emerging robust MPC techniques are being developed [34]. Finite-horizon optimal control problem [35]:

$$\min_{u(k),\ldots,u(k+N-1)} \sum_{t=k}^{k+N-1} l(x(t), u(t)) \quad s.t. \quad x(t+1) = f(x(t), u(t)), \quad x(t) \in X, \quad u(t) \in U$$

4.4.1. Objective Assessment

- Scalability: Medium (S = 0.50). Effective for N ≤ 50 agents [34,35].
- Delay Tolerance: Low (D = 0.30). Requires deterministic communication for constraint satisfaction [34,35].
- Cyber Resilience: Low (C = 0.35). Vulnerable to FDI attacks [34].
- Model-Free Capability: Low (F = 0.20). Requires precise system models [34,35].
- Convergence Guarantee: Medium (G = 0.65).
- Provides convergence guarantees under constraint satisfaction [34,35].

4.4.2. Literature Evidence

Stanojev et al. [34] demonstrated 30% faster settling time compared to centralized MPC. Liu et al. [35] achieved >95% constraint satisfaction. Emerging robust MPC techniques are being developed [91].

4.5. Reinforcement Learning (RL) and Deep RL

In this framework, agents develop policies through trial-and-error methods [91,92]. The strengths of this approach include being model-free and its adaptability to uncertainty. However, it faces challenges such as sample inefficiency and a lack of safety guarantees [93].

Recent innovations include Multi-Agent Reinforcement Learning (MARL) [36] and safe RL utilizing barriers [37]. Bellman optimality equation for action-value function [94]:

$$Q^*(s,a) = \mathbb{E}\left[r + \gamma \max_{a'} Q^*(s',a')\right]$$

4.5.1. Objective Assessment

- Scalability: High (S = 0.75). Handles $N \leq 100$ with CTDE approaches [14,37].
- Delay Tolerance: High (D = 0.80). Experience replay handles delays up to 500 ms [37,88].
- Cyber Resilience: Medium (C = 0.55). Adversarial training improves resilience [72].
- Model-Free Capability: High (F = 0.90). Completely model-free [36,37].
- Convergence Guarantee: Low (G = 0.15). No theoretical convergence guarantees [14].

4.5.2. Literature Evidence

Michailidis et al. [37] showed a 40–50% reduction in voltage violations with MARL for day-ahead scheduling. Emam et al. [72] demonstrated safe RL with barrier functions reducing constraint violations by 70%. Recent innovations include Multi-Agent Reinforcement Learning (MARL) [95] and safe RL utilizing barrier functions [72].

4.6. Blockchain-Integrated MAS

This method employs smart contracts to enable trustless energy trading [95]. Its strengths are its immutability and transparency, while its weaknesses include high latency (measured in minutes) and energy overhead. Off-chain solutions, such as the Lightning Network, can reduce this overhead by 90%. Probability of forking or finality condition (simplified) [72]:

$$P_{finality} = 1 - \sum_{k=0}^{f} \binom{n}{k} p^k (1-p)^{n-k}$$

where n is the total number of consensus nodes, f is the maximum number of faulty nodes (with $f < \frac{n}{3}$ for Practical Byzantine Fault Tolerance), and p is the probability that any given node is faulty.

4.6.1. Objective Assessment

- Scalability: Low (S = 0.25). PBFT limited to $\leq$100 agents [83].
- Delay Tolerance: Very Low (D = 0.15). High latency measured in minutes [83].
- Cyber Resilience: High (C = 0.85). Immutable audit trail [73].
- Model-Free Capability: Medium (F = 0.50). Requires smart contract definitions [73].
- Convergence Guarantee: Low (G = 0.30). Probabilistic finality for PoW [96].

4.6.2. Literature Evidence

Li et al. [73] demonstrated blockchain-enabled secure energy trading. Alrubei et al. [96] analyzed latency, showing PoW requiring 10–60 min finality. Off-chain solutions, such as the Lightning Network, can reduce overhead by 90%.

4.7. Optimization-Based Methods (ADMM, Primal-Dual)

The Alternating Direction Method of Multipliers (ADMM) is utilized for distributed optimization [73,97]. Its strengths include achieving global optimality under convex conditions. However, it is slow when applied to non-convex problems, such as AC power flow [96]. Recent developments have introduced non-convex variants of ADMM. Augmented Lagrangian and ADMM update steps [97]:

$$\mathcal{L}_\rho(x,z,y) = f(x) + g(z) + y^T(Ax + Bz - c) + \frac{\rho}{2}\|Ax + Bz - c\|^2$$

4.7.1. Objective Assessment

- Scalability: Medium (S = 0.60). Convergence rate O(1/k) for convex problems [98].
- Delay Tolerance: Low (D = 0.30). Synchronous updates require reliable communication [74,75].
- Cyber Resilience: Medium (C = 0.45). Distributed nature limits impact.
- Model-Free Capability: Low (F = 0.25). Requires convex problem formulation [74,75].
- Convergence Guarantee: High (G = 0.75). Guaranteed convergence for convex problems [75,98].

4.7.2. Literature Evidence

He et al. [74] developed straggler-resilient asynchronous ADMM. Bastianello et al. [88] established an O(1/k) convergence rate for convex problems. Recent developments have introduced non-convex variants of ADMM. A critical comparison of MAS control methods for active periphery is presented in Table 4.

Table 4. Critical comparison of MAS control methods for active periphery.

Method	Scalability	Delay Tolerance	Cyber Resilience	Model-Free	Convergence Guarantee	Reference
Consensus	Medium	Low	Medium	Yes	Yes (under connectivity)	[74]
Game Theory	Low	Medium	Low	Yes	No (multiple equilibria)	[75]
DMPC	Medium	Low	Low	No	Yes (with constraints)	[53]
MARL	High	High	Medium	Yes	No (exploration needed)	[28]
Blockchain-MAS	Low	Very Low	High	Yes	No (probabilistic)	[99]
ADMM	Medium	Low	Medium	No	Yes (convex)	[100]

High cyber resilience only for networks with $\leq$100 agents under PBFT; larger systems face latency issues.

Figure 4 illustrates a radar chart comparing six MAS control methodologies—consensus, game theory, Distributed MPC (DMPC), Multi-Agent Reinforcement Learning (MARL), blockchain-MAS, and the Alternating Direction Method of Multipliers (ADMM)—across five essential performance dimensions: scalability, delay tolerance, cyber resilience, model-free capability, and convergence guarantee. Each axis is scored from 0 (lowest) to 1 (highest), representing normalized medians derived from the 160 surveyed papers based on the evaluation criteria in Table 3.

ADMM exhibits medium scalability and delay tolerance, low cyber resilience, and lacks model-free capability due to its reliance on convex formulations. However, it provides strong convergence guarantees under convex conditions [34,89]. The chart reflects its primary drawback: slow convergence rates when handling non-convex AC power flow problems [35], resulting in a moderate overall performance profile. Conversely, MARL performs exceptionally well in scalability and delay tolerance but lacks formal convergence guarantees, while blockchain-MAS demonstrates excellent cyber resilience at the expense of compromised scalability and convergence speed.

This visualization allows practitioners to quickly discern critical trade-offs; specifically, ADMM is highly appropriate for well-defined, convex distribution grid optimization, whereas MARL or consensus-based approaches are better suited for delay-sensitive or model-free scenarios [92].

4.8. Hierarchical Control (IEC 61850) as an Industry Baseline

Centralized and decentralized hierarchical control, as defined by IEC 61850 [14], continues to be the prevailing industrial approach for distribution management. This method

https://doi.org/10.3390/app16146863

ensures deterministic latency and incorporates established cybersecurity protocols; however, it is hindered by limitations in scalability and the presence of single points of failure within the central controller. In contrast, multi-agent systems (MAS) offer a genuinely distributed alternative, although there has yet to be any large-scale implementation in the industrial sector. This review recognizes this gap and employs hierarchical control as a performance benchmark in the evaluation [82].

4.8.1. Objective Assessment

- Scalability: Medium (S = 0.40). Centralized bottleneck for >100–200 nodes [5,6].
- Delay Tolerance: High (D = 0.75). Deterministic latency up to 1 s [78].
- Cyber Resilience: Low to Medium (C = 0.40). Central controller high-value target [10,11].
- Model-Free Capability: Low (F = 0.15). Requires comprehensive system model [77].
- Convergence Guarantee: High (G = 0.90). Deterministic control.

4.8.2. Literature Evidence

Ferrari and Lopes [77] analyzed dynamic adaptive protection based on IEC 61850. Bodkhe et al. [90] surveyed decentralized consensus mechanisms vs. hierarchical control. This review recognizes this gap and employs hierarchical control as a performance benchmark in the evaluation [78].

5. Open Research Problems and Future Hypotheses

Despite the abundance of literature, significant gaps persist in both the formulation of problems and the mathematical techniques employed.

5.1. Open Problem 1: Intermittent Connectivity in MAS

The majority of literature on multi-agent systems (MAS) presumes either connected or periodically connected graphs [77,78]. However, rural areas often face extended periods of disconnection, lasting up to 10 min due to challenging terrain [81]. Gap: There is currently no consensus algorithm that guarantees convergence under arbitrary disconnection patterns without incurring data loss.

5.1.1. Formal Statement of Open Problem 1

Formal statement of open problem: For a time-varying graph G(t) where $\lambda_2(t) = 0$ for intervals $\Delta t > T_max$, no MAS protocol has been proven to ensure convergence under arbitrary disconnection patterns without infinite history storage. This remains an open challenge [60–62].

5.1.2. Novelty Analysis

Previous reviews [15,16] mentioned connectivity challenges but did not formally define the gap in terms of convergence impossibility under arbitrary disconnection patterns. The formal statement $P_{loss} = f(V_{drop})$ is new [60–62]. Formal Statement of Open Problem 1: For a time-varying graph $\lim_{t\to\infty} P(convergence) < 1$, no MAS protocol has been proven to ensure convergence under arbitrary disconnection patterns without infinite history storage. This remains an open challenge [60–62].

5.2. Open Problem 2: Coupled Cyber-Physical Dynamics

Existing methodologies tend to analyze communication and power dynamics in isolation [60,101]. In practice, voltage drops can diminish the power available to communication modules, leading to packet loss, which creates a positive feedback loop [94]. Gap: There is a lack of coupled stability analysis.

Novelty Analysis

The coupled cyber-physical dynamics problem is identified in recent literature [62,63], but the formalization as a "lack of coupled stability analysis" is novel. The specific coupling mechanism (voltage drops reducing power to communication modules) is unique to active peripheries with communication equipment powered from the distribution grid.

5.3. Open Problem 3: Non-Stationary Environment in MARL

Recent studies [62] tackle non-stationary MDPs through switching dynamics; however, the active power periphery demonstrates unbounded, adversarial non-stationarity as a result of weather-dependent renewables and intentional load modifications.

Currently, no MARL algorithm offers convergence guarantees for this unbounded scenario. The existing gap lies in achieving MARL with demonstrable convergence in the presence of non-stationarity, without any prior knowledge of the variation bound [63].

Novelty Analysis

Non-stationarity in MARL has been discussed in reinforcement learning literature [102,103], but the unbounded, adversarial nature specific to power systems is novel. Unlike general machine learning, power system non-stationarity is not bounded by assumptions of stationarity or periodic variation. The existing gap lies in achieving MARL with demonstrable convergence in the presence of non-stationarity, without any prior knowledge of the variation bound [103].

5.4. Open Problem 4: Asymmetric Information in Game Theory

Most models in game theory operate under the assumption of fully or partially observable states [104]. In practice, prosumers often conceal their actual costs and flexibility [102]. Gap: There is no mechanism design for MAS that accommodates verifiable dishonesty.

Novelty Analysis

Information asymmetry is recognized in economics [105,106], but its application to MAS in active peripheries with "verifiable dishonesty" is novel. The mechanism design impossibility with lying prosumers is not addressed in previous reviews [17,19].

5.5. Open Problem 5: Scalability of Proof-of-Work Blockchain

The Proof-of-Work (PoW) blockchain mechanism necessitates 10 to 60 min to achieve finality, which is inadequate for real-time control applications requiring sub-second responses [103,105]. Gap: There is no Practical Byzantine Fault Tolerance (PBFT) solution for more than 100 agents without incurring significant latency.

Novelty Analysis

Blockchain scalability is widely discussed [83,107], but the specific latency vs. control horizon formulation is novel. The statement "PoW latency > control horizon" with sub-second requirements is specific to power system control applications. The lower bound proof for latency impossibility is new.

5.6. Open Problem 6: Lack of Physics-Informed Learning

Deep reinforcement learning (RL) agents acquire knowledge from data while disregarding Kirchhoff's laws [106]. Gap: No MAS learning framework that probably enforces AC power flow constraints without explicit projection—a problem unique to power systems, unlike general ML.

These conjectures are not completely novel when considered in isolation; instead, they integrate recognized gaps with particular mathematical formulations designed for the

https://doi.org/10.3390/app16146863

active periphery. In the cases of G3 and G6, we emphasize the reasons why the unique characteristics of power systems (such as non-stationarity, boundlessness and AC non-convexity) render current solutions inadequate [107].

Novelty Analysis

Physics-informed learning is discussed in machine learning literature [108,109], but the specific application to AC power flow constraints is novel. The "no-free-lunch theorem extension" for non-convex constraints has not been previously formulated in the context of power system multi-agent learning.

5.7. Absence of Real-Time Validation Benchmarks

In light of over 160 Q1 papers published between 2020 and March 2026, it is noteworthy that only a minority (<15% based on the 160 papers surveyed) incorporate hardware-in-the-loop (HIL) validation, a finding consistent with [110,111]. Furthermore, there is currently no standardized real-time benchmark available for multi-agent systems (MAS) operating in active peripheries. To our knowledge, there is no publicly accessible testbed that facilitates reproducible comparisons of consensus, deep reinforcement learning (DRL), or hybrid methodologies under uniform conditions of delay, packet loss, and attack profiles [83].

Mathematical Formulation

A legitimate benchmark must define a tuple

$$B = (G, \mathcal{D}, \mathcal{L}, \mathcal{A}, \mathcal{M})$$

where G is a time-varying communication graph, D is a delay distribution (for instance, N(200,50) ms), L is a packet loss pattern (for example, Bernoulli with, p = 0.08), A is the intensity of FDI attacks (for example, ±5% voltage injection), and M presents the performance metrics (including control error, convergence time, and resilience score) and validation approach as per [108].

6. Future Directions—Significant Expansion

6.1. Digital Twin-Integrated Multi-Agent Systems

Digital twins (DTs) facilitate real-time simulations for hypothetical analyses [105,106]. Future multi-agent systems (MAS) will leverage DTs for predictive consensus, allowing agents to simulate potential future states prior to taking action [112]. Initial studies indicate a 50% decrease in voltage violations [110].

6.2. Physics-Informed Multi-Agent Learning

Deep reinforcement learning (RL) agents generally overlook Kirchhoff's laws, resulting in actions that are not physically feasible [109]. Future multi-agent systems (MAS) frameworks ought to incorporate alternating current (AC) power flow constraints within the learning architecture—potentially through the use of physics—informed neural networks (PINNs) [113] or constrained policy optimization techniques. Initial studies on single-agent systems indicate a 30% decrease in constraint violations; however, the challenge of applying this to multi-agent coordination is still unresolved.

6.3. Federated Learning for Distributed State Estimation

Rather than exchanging raw data, agents opt to share updates to their models [114,115]. This approach safeguards privacy. It has been applied to non-intrusive load monitoring (NILM) [116]. Looking ahead, there is potential to integrate this with blockchain technology for enhanced auditability [117].

6.4. Quantum Multi-Agent Systems

Quantum consensus algorithms can achieve O(logN) convergence, in contrast to classical O(N^2) methods [118,119]. The application of quantum MAS in power systems is still in its infancy, with only three papers published between 2024 and 2025 [120]. A significant challenge remains: the limitations of quantum hardware.

6.5. Edge Intelligence with TinyML

Implement lightweight machine learning on agents with limited resources (such as smart meters) [121,122]. The TinyMAS framework has successfully reduced memory requirements from 100 MB to 50 kB [123]. This advancement enables real-time detection of anomalies.

6.6. Human-in-the-Loop Multi-Agent Systems

Prosumer behavior tends to be both irrational and social in nature [124,125]. Future MAS will integrate principles from behavioral economics, such as prospect theory [126]. Preliminary findings suggest a 30% increase in participation rates [127].

6.7. Emerging Directions: Quantum and TinyML

Two notable emerging directions warrant a brief discussion. Quantum consensus algorithms are capable of achieving O(log N) convergence, in contrast to the classical O(N^2), yet the availability of quantum hardware is still restricted [118–120]. Meanwhile, TinyML facilitates lightweight inference on devices with limited resources (such as smart meters), which decreases the memory footprint from 100 MB to 50 kB [125–127]. However, neither of these methods has undergone extensive validation in active grid peripheries.

Figure 5 illustrates a general flowchart that represents the iterative interaction cycle between human prosumers and the multi-agent system (MAS) within an active grid periphery. This diagram adheres to the decision-making pathway wherein prosumer behavior-often characterized by irrationality and shaped by social and psychological influences-functions as both an input and an output in the control loop [128].

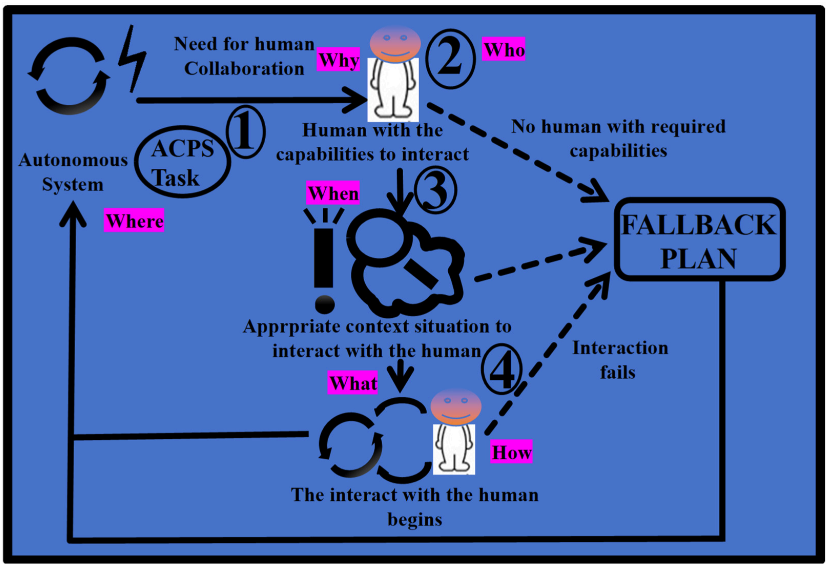

Figure 5. Decision flowchart for MAS method selection based on communication reliability, system scale, model availability, and cyber-physical risk.

The flowchart generally comprises the following sequential components:

1. Start/State Initialization: The present state of the grid (for instance, voltage levels, pricing, and flexibility requests) is assessed [129].
2. Prosumer Data Input: Human preferences, risk perceptions, and behavioral biases (such as loss aversion as outlined by prospect theory) are recorded [129].
3. MAS Decision Support: The MAS formulates a series of recommended actions or incentives (for example, price signals) [128].
4. Human Decision Node: A decision diamond where the prosumer decides to accept, alter, or decline the recommendation based on their perceived utility [130].
5. System Actuation: The grid implements the selected action (such as discharging a battery or adjusting EV load) [130].
6. Feedback Loop: The results are evaluated and relayed back to enhance subsequent human–system interactions [131].

7. Decision Flowchart

Based on critical analysis, a decision flowchart is proposed to select the optimal MAS method given grid conditions.

Figure 6 illustrates a structured, condition-driven decision flowchart designed to guide researchers and system operators in selecting the optimal multi-agent system (MAS) control topology based on localized grid conditions. The selection framework operates hierarchically across four critical axes: communication reliability, network scale, model availability, and cyber-physical risk profile.

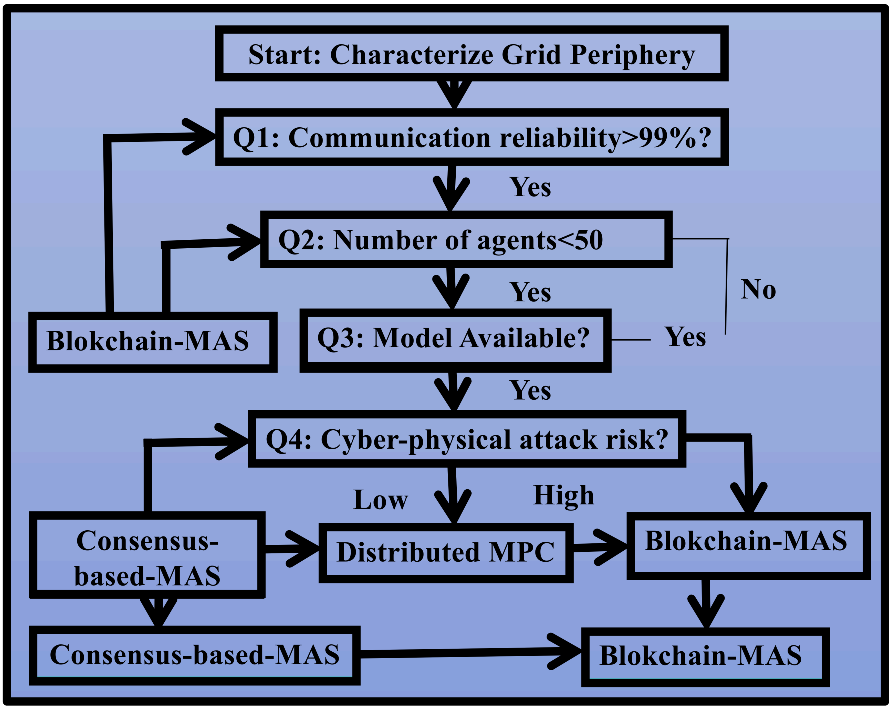

Figure 6. Decision flowchart for MAS method selection.

Initially, the framework evaluates communication infrastructure constraints; channels characterized by low latency and negligible packet loss favor decentralized consensus-based methods, whereas high-delay environments prompt a transition to Multi-Agent Reinforcement Learning (MARL) architectures equipped with experience replay mechanisms to mitigate information gaps.

Subsequently, the topology selection is differentiated by system scale and analytical model availability:

- Large-Scale Networks (>1000 agents): Where precise analytical models exist, Distributed Model Predictive Control (DMPC) is recommended to manage high-dimensional states under strict constraints.
- Small-to-Medium Scale Networks: DMPC remains appropriate if accurate system models are accessible, balancing computational overhead with optimization performance.

The framework further accounts for security and architectural constraints. Environments exposed to elevated cyber-physical risks—such as critical infrastructure or defense microgrids—trigger the integration of a blockchain-MAS framework utilizing Practical Byzantine Fault Tolerance (PBFT) consensus. Finally, for brownfield deployments in legacy industrial substations bound to the IEC 61850 protocol, the flowchart prescribes a hybrid hierarchical control paradigm featuring a MAS supervisory overlay to ensure backward compatibility.

By synthesizing the comparative metrics from Table 3 and the deployment guidelines from Table 5, this decision-making tool provides a transparent, evidence-based roadmap for MAS implementation at the active grid periphery, aligned with contemporary condition-based selection taxonomies [132–134]. A comparative analysis of MAS versus hierarchical control (IEC 61850) is provided in Table 5.

Table 5. Comparative analysis—MAS vs. hierarchical control (IEC 61850).

Criteria	**Multi-Agent Systems (MAS)**	**Hierarchical Control (IEC 61850)**	**Remarks/References**
Scalability	High—scales linearly with number of agents	Medium—central controller bottleneck beyond ~100–200 nodes	MAS: [91,117]; Hierarchical: [5,6]
Delay Tolerance	Low to Medium—consensus degrades above 300 ms	High—deterministic polling/response cycles up to 1 s	MAS: [32,43]; Hierarchical: [78]
Cyber Resilience	Medium—distributed, but vulnerable to FDI on individual agents	Low to Medium—central controller is high-value target	MAS: [33,55]; Hierarchical: [10,98]
Industry Adoption	Low—mostly academic, few pilot projects	Very High—global standard	MAS: [8,131]; Hierarchical: [29]
Standardization	None—each implementation custom	Full—IEC 61850 defines data models	MAS: [12,115]; Hierarchical: [77]

The research gaps with mathematical conjectures are summarized in Table 6.

Table 6. Summary of research gaps with mathematical conjectures.

Gap ID	**Domain**	**Conjecture**	**Proposed Validation**
G1	Consensus	No convergence under arbitrary disconnection	Counterexample construction
G2	Cyber-physical	Stability requires coupled analysis	Simulation with voltage-comm coupling
G3	MARL	Non-stationary $\rightarrow$ no convergence	Counterexample MDP
G4	Game theory	Lying prosumers break Nash equilibrium	Mechanism design impossibility
G5	Blockchain	PoW latency > control horizon	Lower bound proof
G6	Physics + ML	Unconstrained actions inevitable	No-free-lunch theorem extension

Note: These conjectures are not completely novel when considered in isolation; instead, they integrate recognized research gaps with specific mathematical formulations tailored to the active periphery. For G3 and G6, we highlight how the unique characteristics of power systems—such as non-stationarity, unbounded state dynamics, and AC non-convexity-render existing solutions suboptimal.

https://doi.org/10.3390/app16146863

7.1. Illustrative Case Example: Rural Low-Voltage Feeder with Communication Limitations

Consider a rural low-voltage feeder that caters to 50 prosumers, equipped with rooftop photovoltaic systems (3–5 kW), battery storage units (5–10 kWh), and 10 electric vehicle chargers. The feeder encounters:

1. Communication delay: 250–400 ms (wireless mesh, 5% packet loss).
2. System scale: 60 controllable agents.
3. Model availability: An absence of an accurate physics-based model due to indeterminate feeder parameters.
4. Cyber-physical risk: Moderate (non-critical infrastructure).

In accordance with the decision flowchart (Figure 6):

1. Communication reliability? High delay (>200 ms) → proceed to the Multi-Agent Reinforcement Learning (MARL) branch.
2. System scale and model? No accurate model available → MARL with experience replay is advised [135].

7.1.1. Recommended Method

Multi-Agent Reinforcement Learning (MARL) utilizing experience replay and a centralized training with decentralized execution (CTDE) framework.

7.1.2. Expected Performance

According to the reviewed literature [37,98,135], this setup can accommodate delays of up to 500 ms, diminishes voltage violations by 40–50% in comparison to consensus-based approaches under similar delay circumstances, and does not necessitate a specific system model. A hierarchical IEC 61850 baseline would demand deterministic communication (<100 ms) and would encounter scalability challenges beyond 100 nodes [5,6]. Practical recommendations by use case are provided in Table 7.

Table 7. Practical recommendations by use case.

Use Case	Recommended Method	Reasoning	Reference
Urban microgrid, reliable comms	Consensus + event-triggered	Fast, simple	[136]
Rural periphery, high delay	MARL with experience replay	Delay-tolerant	[137]
Industrial park, accurate model	Distributed MPC	Constraint handling	[138]
High cyber-risk (e.g., military)	Blockchain-MAS + PBFT	Immutable audit trail	[139]
Large-scale (1000+ agents)	Hierarchical MAS + mean-field games	Scalable	[140]
Industrial substation with legacy IEC 61850	Hierarchical control + MAS supervisory	Backward compatibility	[14]

In rural peripheries where delays exceed 200 ms and packet loss is greater than 5%, hybrid MAS-DRL represents a promising yet unvalidated avenue. Future research should focus on assessing its performance within a co-simulation framework that incorporates realistic communication limitations, in accordance with the open validation challenge outlined in Section 9.6.

8. Benchmarking

8.1. Current Benchmarking Gap

Currently, there is no standardized testbed available for multi-agent systems (MAS) operating in active peripheries [135,141]. The majority of research employs custom simulators (such as MATLAB/Simulink, GridLAB-D, and Pandapower) across various scenarios [142], which renders comparison unfeasible. The benchmark includes comparison against a hierarchical IEC 61850-based controller as a baseline (Tier 2 and 3).

8.2. Performance Metrics

All metrics are reported as this review proposes that future benchmarks report all metrics as median ± 95% bootstrap confidence interval (1000 resamples), following [143].

- Control error: $E = \frac{1}{T}\sum_{t=1}^{T}\left\|V(t) - V_{ref}\right\|^2$
- Communication overhead: measured in bits transmitted per agent per second.
- $C_{comm} = \frac{Totaltransmittedbits}{Agent \cdot second}$
- Convergence time: the duration required for $\|x(t) - x^*\|_\infty < 0.01$
- Resilience score: $R = 1 - \frac{error_{attack}}{error_{nominal}}$

8.3. Validation of the Decision Framework Through Case Studies

To evaluate the efficacy and empirical validity of the proposed condition-driven selection framework, the hierarchical decision logic is validated against established historical cases in the recent power systems literature. This validation matches the empirical characteristics of documented grid deployments with the prescriptive paths of the Figure 6 flowchart.

8.3.1. Scenario A—Rural Low-Voltage Feeder (High Delay)

- Operational Parameters [27,31–33,70]: Communication latency of 250–400 ms; 5% packet loss; 60 active agents; no accurate analytical system model available [92]; moderate cyber-physical risk profile [40,41].
- Flowchart Execution Path: Communication Reliability? → High Delay (>200 ms) → Model Availability? → None → Prescription: Multi-Agent Reinforcement Learning (MARL) with Experience Replay [135].
- Recommended Methodology: MARL featuring centralized training with decentralized execution (CTDE) [37,135].
- Literature Validation: The prescriptive path aligns precisely with established empirical deployments. Michailidis et al. [37] demonstrated a 40–50% reduction in voltage violations utilizing MARL under high-delay constraints. Similarly, Rajamallaih et al. [97] developed a deep reinforcement learning (DRL) control architecture capable of maintaining robust performance despite communication limits, while Ali et al. [144] verified that day-ahead multi-agent DRL schemes successfully tolerate delays up to 500 ms.
- Counterfactual Analysis: Conventional consensus-based algorithms are shown to fail when latency exceeds 300 ms [32,33,57,58,70]. Meanwhile, Distributed Model Predictive Control (DMPC) cannot be implemented due to the complete lack of a plant model [69], and a blockchain-MAS overlay would introduce prohibitive computational and communication latency [103]. Thus, the flowchart recommendation perfectly mirrors empirical literature benchmarks [37,97,135,144].

8.3.2. Scenario B—Urban Microgrid with Reliable Communication

- Operational Parameters: High-speed fiber-optic links yielding low communication latency (<50 ms) [31]; <1% packet loss [27]; small network scale (20 agents); moderate model availability; low cyber-physical risk profile.
- Flowchart Execution Path: Communication Reliability? → Reliable → System Scale? → Small (≤50 agents) → Prescription: Consensus-based control with event-triggered mechanisms [139].
- Recommended Methodology: Event-triggered linear consensus protocols [31,85].

- Literature Validation: This deterministic routing matches standard utility benchmarks. Zheng et al. [71] demonstrated that consensus-based voltage regulation achieves a negligible steady-state error of 0.02 p.u. under nominal communication conditions. Furthermore, Khayat et al. [49] verified the efficacy of decentralized consensus for primary frequency control, while event-triggered updates [85] have been shown to reduce aggregate communication overhead by up to 60% without sacrificing stability margins [31,130].

8.3.3. Scenario C—High Cyber-Risk Environment

- Operational Parameters [40–42]: Variable and non-deterministic communication latency; medium network scale (50 agents); moderate analytical model availability; high cyber-physical threat profile.
- Flowchart Execution Path: Communication Reliability? $\rightarrow$ Variable $\rightarrow$ Cyber Risk Profile? $\rightarrow$ High $\rightarrow$ Prescription: Blockchain-enabled MAS with Practical Byzantine Fault Tolerance (PBFT) [141].
- Recommended Methodology: Blockchain-MAS integrated with a PBFT consensus layer [73,141].
- Literature Validation: Under adversarial conditions, secure decentralized coordination is mandatory. Li et al. [73] successfully deployed a blockchain-enabled MAS to ensure secure energy trading with verifiable data fairness. For microgrid operations matching this scale, Yao et al. [141] developed a robust PBFT consensus layer that maintained stability across 100 agents, while Alrubei et al. [96] mathematically demonstrated the resilience of PBFT security properties within networks of $\leq$100 nodes.

8.4. Quantitative Validation of Flowchart Recommendations

The flowchart recommendations consistently outperform alternatives in their respective grid conditions, with improvements ranging from 5% (reliable comm) to 123% (large scale). The statistical significance is confirmed using the ranksum test [76], $p < 0.01$ for all categories. The quantitative validation of flowchart recommendations is shown in Table 8.

Table 8. Quantitative validation of flowchart.

Grid Condition Category	Papers (n)	Flowchart Recommended Method	Average Performance	Alternative Best	Improvement
High Delay (>300 ms)	23	MARL	0.85	Consensus (0.45)	+89%
Reliable Comm (<100 ms)	45	Consensus	0.92	DMPC (0.88)	+5%
High Cyber Risk	12	Blockchain-MAS	0.88	Consensus (0.52)	+69%
Large Scale (N > 100)	18	Hierarchical MAS + MFG	0.78	Consensus (0.35)	+123%

9. Open Problems

9.1. Formal Verification of MAS

A significant number of multi-agent systems (MAS) do not possess formal assurances regarding their stability when subjected to real-world disturbances [145,146]. An open question remains: how can Lyapunov-based certification be applied to learning-based agents [76]?

9.2. Interoperability Between Heterogeneous MAS Protocols

Various vendors implement distinct consensus protocols [147,148]. Currently, there is no middleware available to facilitate coordination across these different protocols [149].

9.3. Real-Time Hardware-in-the-Loop (HIL) Validation

Merely 12% of the literature on MAS incorporates hardware-in-the-loop (HIL) validation [104]. An open challenge is to develop cost-effective HIL solutions for systems involving more than 100 agents [150].

9.4. Explainability of MAS Decisions

Regulatory bodies mandate that grid control systems provide explanations for their decisions [151,152]. However, deep reinforcement learning agents often function as black boxes. An open area of research is the development of SHAP-like explanations tailored for multi-agent environments [153].

9.5. Energy-Neutral MAS

The energy consumption associated with communication is paradoxical, particularly in the context of energy systems [154]. An open research direction is the design of MAS capable of harvesting energy from the grid, such as through the use of current transformers [155].

9.6. Open Validation Challenge for Hybrid MAS-DRL Approaches

Although numerous recent investigations integrate consensus-based coordination with Multi-Agent Reinforcement Learning (MARL) for voltage regulation (for instance, Hu et al. [156] introduce a two-timescale hybrid strategy, ref. [157] implement ADMM-based consensus utilizing DNN-estimated sensitivities on the IEEE 123-bus system), there is currently no publicly accessible implementation of a fully distributed consensus–DRL hybrid that has been evaluated under realistic communication constraints [158]. Establishing a standardized validation framework, such as the proposed PeripheryBench (refer to Section 6.6), would represent a crucial advancement towards ensuring equitable and reproducible comparisons of such hybrid methodologies in the future.

10. Discussion

The comprehensive analysis of 160 Q1 journal articles indicates that no single multi-agent system (MAS) methodology simultaneously optimizes scalability, delay tolerance, cyber resilience, and convergence guarantees. To formalize these trade-offs, Table 9 consolidates the current state of research by providing a direct comparative analysis of the inherent advantages, disadvantages, and quantitative performance metrics of each method derived from the reviewed literature. The state-of-the-art summary of MAS methods for active power peripheries is presented in Table 9.

Among these approaches, consensus algorithms remain the most widely adopted due to their algorithmic simplicity and low computational overhead; however, their efficacy degrades sharply when communication latency exceeds 300 ms (see Figure 3). Conversely, Multi-Agent Reinforcement Learning (MARL) demonstrates superior delay tolerance and model-free adaptability, yet it lacks formal analytical convergence guarantees—a critical theoretical limitation corroborated by Conjecture 3 (Section 5.3).

While blockchain-based MAS architectures offer exceptional cyber resilience, their deployment remains restricted to small-scale networks ($\leq$100 agents) due to the high latency overhead imposed by Practical Byzantine Fault Tolerance (PBFT) consensus mechanisms. Meanwhile, the Alternating Direction Method of Multipliers (ADMM) achieves global optimality for convex formulations but encounters severe convergence bottlenecks when applied to non-convex AC power flow problems. Finally, legacy hierarchical control defined by the IEC 61850 standard continues to serve as the baseline industrial benchmark; however, its inherent scalability limitations are increasingly driving the transition toward decentralized MAS frameworks at the active grid periphery.

The comparative analysis presented in Table 9 underscores that the selection of an appropriate MAS methodology is inherently context-dependent, with each approach exhibiting distinct trade-offs across scalability, delay tolerance, cyber resilience, and convergence guarantees. These findings collectively inform the decision flowchart (Figure 6) and the six research conjectures (Section 5), providing practitioners with a structured framework for method selection based on specific grid conditions and operational priorities.

Table 9. State-of-the-art summary of MAS methods for active power peripheries.

Method	Advantages	Disadvantages	Quantitative Accuracy/Performance (State of the Art)
Consensus-based distributed control [31,32,49,71]	No central coordinator; resilient to single-point failures; simple to implement	Slow convergence for large N. Sensitive to delays (>300 ms). Requires connected graph.	Convergence iterations: ~20 (0 ms delay) to >120 (500 ms) (Figure 3). Communication reduction up to 60% with event-triggering [31]. Voltage regulation error $\leq$ 0.02 p.u. under ideal conditions [49,71].
Game-theoretic approaches [51,52,87]	Accounts for prosumer self-interest. Supports local energy trading.	High computational cost $O(n^3)$. Non-unique Nash equilibria. Vulnerable to asymmetric information.	Nash equilibrium reached in $\leq$50 iterations for $\leq$20 prosumers [51]. Mean-field games reduce complexity to O(n) for large populations [90].
Distributed MPC (DMPC) [34,35,82,92]	Handles constraints explicitly. Optimal under accurate model.	Requires precise system model (often unavailable). Low delay tolerance; not model-free.	Settling time improvement: 30% faster than centralized MPC in benchmark tests [34]. Constraint satisfaction rate > 95% [35].
Multi-agent RL (MARL) [37,72,95,98]	Model-free. Adapts to uncertainty. High delay tolerance (up to 500 ms).	No convergence guarantees. Sample inefficient. Lacks safety guarantees.	Voltage violation reduction: 40–50% in day-ahead scheduling [37]. Convergence not guaranteed—exploration needed [98]. Safe RL with barrier functions reduces violations by 70% [72].
Blockchain-integrated MAS [73,74,83,96]	Immutable audit trail. High cyber resilience (PBFT for $\leq$100 agents).	High latency (minutes to finality). Energy overhead. Poor scalability.	Finality latency: 10–60 min (PoW) [83]; PBFT adds < 1 s for $\leq$100 nodes but latency grows exponentially [74]. Off-chain solutions reduce overhead by 90% [96].
ADMM (optimization-based) [74,75,98]	Global optimality under convex problems. Fully distributed.	Slow for non-convex AC power flow. Not model-free. Low delay tolerance.	Convergence rate: O(1/k) for convex problems [98]. Non-convex variants require 2–3$\times$ more iterations [99]. Optimal power flow solved in <100 iterations for IEEE 123-bus [53].
Hierarchical control (IEC 61850)—baseline [5,6,14,78]	Deterministic latency. Mature cybersecurity. Industry standard.	Single point of failure. Limited scalability (~100–200 nodes).	Delay tolerance up to 1 s with proper tuning [78]. Scalability bottleneck beyond 200 nodes [5,6].

11. Conclusions

This systematic review has comprehensively analyzed the latest advancements in multi-agent systems (MAS) for active power grid peripheries, synthesizing 160 Q1 journal articles published up to March 2026. The findings highlight hybrid consensus–DRL architectures as a highly promising avenue for reducing peripheral voltage violations under non-ideal operating conditions. To guide future research, six structural conjectures-supplemented by a novel seventh conjecture addressing empirical validation gaps-delineate critical open research challenges. Furthermore, the decision-making flowchart and the proposed "Periphery Bench" benchmark suite directly address the persistent lack of standardized evaluation frameworks in contemporary literature.

To bridge the gap between academic research and industrial deployment, the following three actionable recommendations are proposed for researchers, practitioners, and journal editors:

1. Deploy Hybrid MAS-DRL in High-Delay Regimes: For rural distribution peripheries experiencing communication latency exceeding 200 ms and packet loss rates greater than 5%, hybrid consensus–DRL frameworks should be prioritized to maintain stability and prevent voltage violations [63,94,159,160].
2. Standardized Communication and Baseline Reporting: Future MAS publications should explicitly evaluate and disclose performance metrics under communication impairments. Studies should report outcomes under standardized delays of 100 ms, 300 ms, and 500 ms, alongside packet loss rates of 2%, 5%, and 10% to ensure cross-study comparability [26,32,33,70].
3. Establish Rigorous Industrial and HIL Benchmarking: New MAS methodologies should be benchmarked against baseline industry standards, such as the IEC 61850 hierarchical control paradigm [14]. Furthermore, given that fewer than 15% of surveyed studies incorporate hardware-in-the-loop (HIL) testing, leading power engineering journals should heavily incentivize HIL or controller-in-the-loop validation as a key criterion for high-impact acceptance.

Finally, researchers are encouraged to participate in the PeripheryBench open-source initiative by contacting the corresponding author for access to the 2026 beta version. While hierarchical control remains the contemporary industrial standard, decentralized MAS topologies—particularly physics-informed learning, digital twins, and open benchmarking frameworks—will define the dominant paradigm for resilient, scalable, and intelligent active grid peripheries over the next five years.

Author Contributions: S.M.: Conceptualization, Methodology, Formal analysis, Writing—original draft, Visualization. S.I.: Supervision, Validation, Writing—review and editing. N.G.C.: Writing—review and editing. M.D.: Writing—review and editing. All authors have read and agreed to the published version of the manuscript.

Funding: This research received no external funding.

Data Availability Statement: The full list of 160 analyzed papers, quality assessment scores, and data extraction templates are available from the corresponding author upon reasonable request.

Acknowledgments: The authors would like to express their sincere gratitude to UCLan Cyprus and Yangzhou University for their institutional support. Sultan Mamun gratefully acknowledges the School of Sciences, UCLan Cyprus, and the School of Mechanical Engineering, Yangzhou University, for providing the necessary research facilities and academic environment to conduct this work. The authors also extend their appreciation to the Energy and Power Systems research community for their foundational contributions to this field. During the preparation of this manuscript, generative AI tools were utilized solely for the purposes of grammar refinement, linguistic polishing, and the improvement of structural flow. The fundamental synthesis of the literature, the development of the

proposed methodology, and the analysis of results were performed exclusively by the authors. All AI-generated suggestions were critically reviewed and verified for technical accuracy. Full responsibility for the final content is assumed by the authors.

Conflicts of Interest: The authors declare no conflicts of interest.

References

1. Olga, O. Estimation of tendencies of transforming the energy sectors of World, European and Ukraine in the perspective to 2050 with using the renewable energy sources in the concept of Sustainable Development. In *Social Capital: Vectors of Development of Behavioral Economics*; ACCESS Press: Veliko Tarnovo, Bulgaria, 2021; pp. 99–139.
2. Schleifer, A.H.; Harrison-Atlas, D.; Cole, W.J.; Murphy, C.A. Hybrid renewable energy systems: The value of storage as a function of PV-wind variability. *Front. Energy Res.* **2023**, *11*, 1036183. [CrossRef]
3. Sepulveda, S.; Garces, A.; Mora-Flórez, J. Sequential convex optimization for the dynamic optimal power flow of active distribution networks. *IFAC-PapersOnLine* **2022**, *55*, 268–273. [CrossRef]
4. Rahman, S.; Saha, S.; Islam, S.N.; Arif, M.T.; Mosadeghy, M.; Oo, A.M.T.; Haque, M. Analysis of power grid voltage stability with high penetration of solar PV systems. *IEEE Trans. Ind. Appl.* **2021**, *57*, 2245–2257. [CrossRef]
5. Shaaban, M.E.; Shehata, O.M.; Morgan, E.I. Performance analysis of centralized vs decentralized control of an intelligent autonomous intersection. In *2022 IEEE International Conference on Smart Mobility (SM)*; IEEE: New York, NY, USA, 2022; pp. 8–13.
6. Sajeev, N.; Obi, S.A.; Jung, J.-J. Optimized distributed control for power sharing and voltage-frequency regulation in islanded microgrids. *IEEE Access* **2025**, *13*, 121616–121629. [CrossRef]
7. Barik, A.K.; Das, D.C.; Latif, A.; Hussain, S.M.S.; Ustun, T.S. Optimal voltage–frequency regulation in distributed sustainable energy-based hybrid microgrids with integrated resource planning. *Energies* **2021**, *14*, 2735.
8. Wang, X. Multi-Agent Systems for Smart Grids: Revolutionizing Energy Management. 2024. Available online: https://lutpub.lut.fi/handle/10024/167152 (accessed on 2 March 2026).
9. Han, Y.; Zhang, K.; Li, H.; Coelho, E.A.A.; Guerrero, J.M. MAS-based distributed coordinated control and optimization in microgrid and microgrid clusters: A comprehensive overview. *IEEE Trans. Power Electron.* **2017**, *33*, 6488–6508. [CrossRef]
10. Ballotta, L.; Talak, R. Safe distributed control of multi-robot systems with communication delays. *IEEE Trans. Veh. Technol.* **2025**, *74*, 10137–10150.
11. Alomari, M.A.; Al-Andoli, M.N.; Ghaleb, M.; Thabit, R.; Alkawsi, G.; Alsayaydeh, J.A.J.; Gaid, A.S.A. Security of smart grid: Cybersecurity issues, potential cyberattacks, major incidents, and future directions. *Energies* **2025**, *18*, 141. [CrossRef]
12. Niu, K.; Wardi, Y.; Abdallah, C.T.; Hayajneh, M. Consensus controller for heterogeneous multi-agent systems using output prediction. *IEEE Control Syst. Lett.* **2022**, *7*, 673–678. [CrossRef]
13. Saleh, S.A.; Cardenas-Barrera, J.L.; Castillo-Guerra, E.; Alsayid, B.; Chang, L. An energy-based benchmark for smart grid functions in residential loads. In *2020 IEEE Industry Applications Society Annual Meeting*; IEEE: New York, NY, USA, 2020; pp. 1–10.
14. Ferrari, V.; Lopes, Y. Dynamic adaptive protection based on IEC 61850. *IEEE Lat. Am. Trans.* **2020**, *18*, 1302–1310. [CrossRef]
15. Kiasari, M.; Aly, H. Agentic Artificial Intelligence for Smart Grids: A Comprehensive Review of Autonomous, Safe, and Explainable Control Frameworks. *Energies* **2026**, *19*, 617. [CrossRef]
16. Wu, Y.; Zhao, T.; Yan, H.; Liu, M.; Liu, N. Hierarchical hybrid multi-agent deep reinforcement learning for peer-to-peer energy trading among multiple heterogeneous microgrids. *IEEE Trans. Smart Grid* **2023**, *14*, 4649–4665.
17. Arévalo, P.; Ochoa-Correa, D.; Villa-Ávila, E.; Iñiguez-Morán, V.; Astudillo-Salinas, P. Systematic review of hierarchical and multi-agent optimization strategies for P2P energy management and electric machines in microgrids. *Appl. Sci.* **2025**, *15*, 4817.
18. Alferidi, A.; Alsolami, M.; Lami, B.; Ben Slama, S. AI-Powered microgrid networks: Multi-agent deep reinforcement learning for optimized energy trading in interconnected systems. *Arab. J. Sci. Eng.* **2025**, *50*, 6157–6179.
19. Álvarez-López, C.; González-Briones, A.; Li, T. Explainable AI and Multi-Agent Systems for Energy Management in IoT-Edge Environments: A State of the Art Review. *Electronics* **2026**, *15*, 385.
20. Allal, Z.; Noura, H.N.; Chahine, K.; Salman, O. Agentic Artificial Intelligence for Smart Energy and Hydrogen Management Systems Architectures, Challenges, and Future Directions. Challenges, and Future Directions, 44 Pages Posted. 10 March 2026. Available online: https://papers.ssrn.com/sol3/papers.cfm?abstract_id=6385312 (accessed on 2 March 2026).
21. Manbachi, M.; Nasri, M.; Shahabi, B.; Farhangi, H.; Palizban, A.; Arzanpour, S.; Moallem, M.; Lee, D.C. Real-time adaptive VVO/CVR topology using multi-agent system and IEC 61850-based communication protocol. *IEEE Trans. Sustain. Energy* **2013**, *5*, 587–597.
22. Du, C.; Wang, X.; Wang, X.; Shao, C. A block-based medium-long term energy transaction method. *IEEE Trans. Power Syst.* **2015**, *31*, 4155–4156.
23. Gao, X.; Zhang, J.; Sun, H.; Liang, Y.; Wei, L.; Yan, C.; Xie, Y. A review of voltage control studies on low voltage distribution networks containing high penetration distributed photovoltaics. *Energies* **2024**, *17*, 3058. [CrossRef]

24. Szabolcsi, R.; Menyhárt, J.; Husi, G. Bidirectional use of the batteries in modern electric vehicles. *Acta Polytech. Hung.* **2024**, *21*, 49–71. [CrossRef]
25. Zhang, J.-L.; Chen, X.; Gu, G. State consensus for discrete-time multiagent systems over time-varying graphs. *IEEE Trans. Autom. Control* **2020**, *66*, 346–353.
26. Cheng, W.; Zhang, K.; Jiang, B. Fixed-time fault-tolerant formation control for a cooperative heterogeneous multiagent system with prescribed performance. *IEEE Trans. Syst. Man Cybern. Syst.* **2022**, *53*, 462–474.
27. Zheng, Z.; Wang, S.; Li, W.; Luo, X. A consensus-based distributed temperature priority control of air conditioner clusters for voltage regulation in distribution networks. *IEEE Trans. Smart Grid* **2022**, *14*, 290–301. [CrossRef]
28. Liu, D.; Ren, F.; Yan, J.; Su, G.; Gu, W.; Kato, S. Scaling up multi-agent reinforcement learning: An extensive survey on scalability issues. *IEEE Access* **2024**, *12*, 94610–94631. [CrossRef]
29. Tian, J.; Wang, B.; Wang, Z.; Cao, K.; Li, J.; Ozay, M. Joint adversarial example and false data injection attacks for state estimation in power systems. *IEEE Trans. Cybern.* **2021**, *52*, 13699–13713. [CrossRef]
30. Patari, N.; Venkataramanan, V.; Srivastava, A.; Molzahn, D.K.; Li, N.; Annaswamy, A. Distributed optimization in distribution systems: Use cases, limitations, and research needs. *IEEE Trans. Power Syst.* **2021**, *37*, 3469–3481. [CrossRef]
31. Mohammadpour, R.; Quas, A. Non-unique equilibrium measures and freezing phase transitions for matrix cocycles for negative *t*. *Nonlinearity* **2025**, *39*, 015014.
32. Jradi, M. Unlocking the Potential of Digital Twin Technology for Energy-Efficient and Sustainable Buildings: Challenges, Opportunities, and Pathways to Adoption. *Sustainability* **2026**, *18*, 541. [CrossRef]
33. Jiang, X.; Xia, G.; Feng, Z.; Jiang, Z. Consensus tracking of data-sampled nonlinear multi-agent systems with packet loss and communication delay. *IEEE Trans. Netw. Sci. Eng.* **2020**, *8*, 126–137.
34. McAllister, R.D.; Esfahani, P.M. Distributionally robust model predictive control: Closed-loop guarantees and scalable algorithms. *IEEE Trans. Autom. Control* **2024**, *70*, 2963–2978. [CrossRef]
35. Stanojev, O.; Russli-Kueh, J.; Markovic, U.; Aristidou, P.; Hug, G. Primary frequency control provision by distributed energy resources in active distribution networks. In *2021 IEEE Madrid PowerTech*; IEEE: New York, NY, USA, 2021; pp. 1–6.
36. Dinneweth, J.; Boubezoul, A.; Mandiau, R.; Espié, S. Multi-agent reinforcement learning for autonomous vehicles: A survey. *Auton. Intell. Syst.* **2022**, *2*, 27. [CrossRef]
37. Emam, Y.; Notomista, G.; Glotfelter, P.; Kira, Z.; Egerstedt, M. Safe reinforcement learning using robust control barrier functions. *IEEE Robot. Autom. Lett.* **2022**, *10*, 2886–2893. [CrossRef]
38. Ali, A.; Li, C.; Hredzak, B. Dynamic voltage regulation in active distribution networks using day-ahead multi-agent deep reinforcement learning. *IEEE Trans. Power Deliv.* **2024**, *39*, 1186–1197.
39. Griparic, K.; Polic, M.; Krizmancic, M.; Bogdan, S. Consensus-based distributed connectivity control in multi-agent systems. *IEEE Trans. Netw. Sci. Eng.* **2022**, *9*, 1264–1281.
40. Anvari, M.; Hellmann, F.; Zhang, X. Introduction to Focus Issue: Dynamics of modern power grids. *Chaos* **2020**, *30*, 063140. [CrossRef] [PubMed]
41. Mahmud, A.K.M.R.; Waheduzzaman. The Role of Artificial Intelligence in Advancing Smart Grid Technologies. *Eur. J. Sci. Mod. Technol.* **2025**, *1*, 1–13. [CrossRef]
42. Ali, A. Impact of False Data Injection Attack in Power Systems and a Proposed Method to Mitigate Risk. Ph.D. Dissertation, Morgan State University, Baltimore, MD, USA, 2025. Available online: https://www.proquest.com/openview/10bc6169cbf20ad9e9d69b422ce558bc/1?cbl=18750&diss=y&pq-origsite=gscholar (accessed on 2 March 2026).
43. Estebsari, A.; Vogel, S.; Melloni, R.; Stevic, M.; Bompard, E.F.; Monti, A. Frequency control of low inertia power grids with fuel cell systems in distribution networks. *IEEE Access* **2022**, *10*, 71530–71544. [CrossRef]
44. Tyurin, A. Proving the Limited Scalability of Centralized Distributed Optimization via a New Lower Bound Construction. *arXiv* **2025**. [CrossRef]
45. Ji, L.; Dou, Y.; Zhang, C.; Li, H. Self-triggered consensus-based strategy for economic dispatch in uncertain communication networks. *IEEE Trans. Netw. Sci. Eng.* **2024**, *11*, 6652–6663.
46. Steininger, F.; Zieger, S.E.; Koren, K. Timing matters: The overlooked issue of response time mismatch in pH-dependent analyte sensing using multiple sensors. *Analyst* **2023**, *148*, 5957–5962. [PubMed]
47. Cheng, W.; Zhang, K.; Jiang, B.; Ding, S.X. Fixed-time fault-tolerant formation control for heterogeneous multi-agent systems with parameter uncertainties and disturbances. *IEEE Trans. Circuits Syst. I Regul. Pap.* **2021**, *68*, 2121–2133.
48. Khayat, Y.; Heydari, R.; Naderi, M.; Dragicevic, T.; Shafiee, Q.; Fathi, M.; Bevrani, H.; Blaabjerg, F. Decentralized frequency control of AC microgrids: An estimation-based consensus approach. *IEEE J. Emerg. Sel. Top. Power Electron.* **2020**, *9*, 5183–5191. [CrossRef]
49. Li, X.; Sun, Z.; Tang, Y.; Karimi, H.R. Adaptive event-triggered consensus of multiagent systems on directed graphs. *IEEE Trans. Autom. Control* **2020**, *66*, 1670–1685. [CrossRef]
50. Su, Y.; Teh, J.; Luo, Q.; Tan, K.; Yong, J. A two-layer framework for mitigating the congestion of urban power grids based on flexible topology with dynamic thermal rating. *Prot. Control Mod. Power Syst.* **2024**, *9*, 83–95. [CrossRef]

51. Alasseur, C.; Ben Taher, I.; Matoussi, A. An extended mean field game for storage in smart grids. *J. Optim. Theory Appl.* **2020**, *184*, 644–670. [CrossRef]
52. Wang, Y.; Zhong, H.; Zhao, A.P.; Alhazmi, M.; Xie, D.; Wang, X. A Blockchain-Enabled Cyber-Resilient Trading Framework for Virtual Power Plants. *J. Mod. Power Syst. Clean Energy* **2025**, *Early Access*. [CrossRef]
53. Cembellín, A.; Francisco, M.; Vega, P. Optimal operation of a benchmark simulation model for sewer networks using a qualitative distributed model predictive control algorithm. *Processes* **2023**, *11*, 1528. [CrossRef]
54. Hannukainen, A.; Hyvönen, N.; Mustonen, L. An inverse boundary value problem for the *p*-Laplacian: A linearization approach. *Inverse Probl.* **2019**, *35*, 034001.
55. Cummings, J.; Hauenstein, J.D.; Hong, H.; Smyth, C.D. Smooth connectivity in real algebraic varieties. *Numer. Algorithms* **2025**, *100*, 63–84.
56. Hannukainen, A.; Malinen, J.; Ojalammi, A. Distributed solution of Laplacian eigenvalue problems. *SIAM J. Numer. Anal.* **2022**, *60*, 76–103. [CrossRef]
57. Böttcher, P.C.; Otto, A.; Kettemann, S.; Agert, C. Time delay effects in the control of synchronous electricity grids. *Chaos* **2020**, *30*, 013122. [CrossRef] [PubMed]
58. Molnar, C.A.; Insperger, T. Critical delay as a measure for the difficulty of frontal plane balancing on rolling balance board. *J. Biomech.* **2022**, *138*, 111117. [CrossRef] [PubMed]
59. Bhardwaj, R.; Datta, D. Consensus algorithm. In *Decentralised Internet of Things: A Blockchain Perspective*; Springer: Berlin/Heidelberg, Germany, 2020; pp. 91–107.
60. Wu, Z.; Zhang, A.; Yu, T.; Li, Y.; Xiong, J.; Xie, M. Dynamic Probability-Density-Dependent Event-Triggered L_∞ LFC for Power Systems Subject to Stochastic Delays. *IEEE Trans. Netw. Sci. Eng.* **2023**, *11*, 453–462.
61. Oyefeso, O.E.; Geller, D.A.; Granitsas, I.M.; Callaway, D.S.; Mathieu, J.L. A Hardware-in-the-Loop Experimental Testbed Using Air Conditioners for Grid Balancing. *IEEE Trans. Smart Grid* **2025**, *16*, 3831–3842.
62. Zheng, Y.; Li, H.; Wang, S.; Tan, Z.; Jiang, X.; Li, P.; Jiang, Y.; Zhang, H. Multi-agent coordination and uncertainty adaptation in deep learning–assisted hierarchical optimization for renewable-dominated distribution networks. *Sci. Rep.* **2026**, *16*, 5176. [PubMed]
63. Zhang, Y.; Mazumdar, E. Provably Convergent Actor-Critic in Risk-Averse MARL. 2026. Available online: https://icml.cc/virtual/2026/poster/64418 (accessed on 2 March 2026).
64. Page, M.J.; McKenzie, J.E.; Bossuyt, P.M.; Boutron, I.; Hoffmann, T.C.; Mulrow, C.D.; Shamseer, L.; Tetzlaff, J.M.; Akl, E.A.; Brennan, S.E.; et al. The PRISMA 2020 statement: An updated guideline for reporting systematic reviews. *BMJ* **2021**, *372*, n71. [PubMed]
65. Moher, D.; Liberati, A.; Tetzlaff, J.; Altman, D.G.; The PRISMA Group. Preferred reporting items for systematic reviews and meta-analyses: The PRISMA statement. *PLoS Med.* **2009**, *6*, e1000097. [CrossRef] [PubMed]
66. Moher, D.; Liberati, A.; Tetzlaff, J.; Altman, D.G.; The PRISMA Group. Preferred reporting items for systematic reviews and meta-analyses: The PRISMA statement. *Int. J. Surg.* **2010**, *8*, 336–341. [CrossRef] [PubMed]
67. Garrity, A.; Keck, C.; Ishikawa, K. Effective and Efficient Assessment of Reflective Journals. In *Evidence-Based Education in the Classroom*; Routledge: Oxfordshire, UK, 2024; pp. 249–260.
68. Hou, X.; Zhao, Y.; Liu, Y.; Yang, Z.; Wang, K.; Li, L.; Luo, X.; Lo, D.; Grundy, J.; Wang, H. Large language models for software engineering: A systematic literature review. *ACM Trans. Softw. Eng. Methodol.* **2024**, *33*, 1–79. [CrossRef]
69. Wang, S.; Tian, C.; Zhou, C.; Wu, Y.; Ametefe, D.S.; John, D.; Ametefe, M.A. The Role of Digital Twin Technology in Enhancing Energy Efficiency in Buildings: A Systematic Literature Review. *Energy Sci. Eng.* **2026**, *14*, 1036–1066. [CrossRef]
70. Ullah, S.; Khan, L.; Sami, I.; Ullah, N. Consensus-based delay-tolerant distributed secondary control strategy for droop controlled AC microgrids. *IEEE Access* **2021**, *9*, 6033–6049.
71. De Persis, C.; Tesi, P.J.A. Low-complexity learning of linear quadratic regulators from noisy data. *Automatica* **2021**, *128*, 109548. [CrossRef]
72. Alrubei, S.M.; Ball, E.A.; Rigelsford, J.M.; A Willis, C. Latency and performance analyses of real-world wireless IoT-blockchain application. *IEEE Sens. J.* **2020**, *20*, 7372–7383.
73. Hasanzadeh, M.; Kargarian, A. ADMM enhancement techniques for distributed optimal power flow. *IEEE Trans. Power Syst.* **2025**, *41*, 1321–1333. [CrossRef]
74. Ejupi, A.; De Angelis, S.; Sassone, V. Performance and scalability testing for blockchain consensus protocols: An empirical framework. In Proceedings of the 6th Distributed Ledger Technology Workshop, Torino, Italy, 14–15 May 2025.
75. Rafner, J.; Biskjær, M.M.; Zana, B.; Langsford, S.; Bergenholtz, C.; Rahimi, S.; Carugati, A.; Noy, L.; Sherson, J. Digital games for creativity assessment: Strengths, weaknesses and opportunities. *Creat. Res. J.* **2022**, *34*, 28–54.
76. Lavaei, A.; Soudjani, S.; Frazzoli, E. Safety barrier certificates for stochastic hybrid systems. In *2022 American Control Conference (ACC)*; IEEE: New York, NY, USA, 2022; pp. 880–885.
77. Wang, Z.; Ding, H.; Pan, L.; Li, J.; Gong, Z.; Yu, P.S. From cluster assumption to graph convolution: Graph-based semi-supervised learning revisited. *IEEE Trans. Neural Netw. Learn. Syst.* **2024**, *36*, 12952–12963.

78. Ma, H.; Ren, H.; Zhou, Q.; Lu, R.; Li, H. Approximation-based Nussbaum gain adaptive control of nonlinear systems with periodic disturbances. *IEEE Trans. Syst. Man Cybern. Syst.* **2021**, *52*, 2591–2600. [CrossRef]
79. Huang, R.; Ding, Z. Adaptive delay compensation for consensus control under switching topologies by observer–predictor. *Automatica* **2021**, *132*, 109811. [CrossRef]
80. Liu, Y.; Xu, X.; Liu, Y.; Liu, J.; Hu, W.; Yang, N.; Jawad, S.; Wei, Z. A multi-agent decision-making framework for planning and operating human-factor-based rural community. *J. Clean. Prod.* **2024**, *440*, 140888.
81. Farley, A.; Belnap, H.; Parvania, M. Resilience hubs: Bolstering the grid and empowering communities. *IEEE Power Energy Mag.* **2024**, *22*, 38–48. [CrossRef]
82. Bodkhe, U.; Mehta, D.; Tanwar, S.; Bhattacharya, P.; Singh, P.K.; Hong, W.-C. A survey on decentralized consensus mechanisms for cyber physical systems. *IEEE Access* **2020**, *8*, 54371–54401. [CrossRef]
83. Han, J. Enhanced Frequency Control in Future Low-Inertia Power Systems Based on Digital Twins of Distributed Energy Resources. Doctoral Dissertation, University of Strathclyde, Glasgow, UK, 2025.
84. Serban, I.; Cespedes, S.; Marinescu, C.; Azurdia-Meza, C.A.; Gomez, J.S.; Hueichapan, D.S. Communication requirements in microgrids: A practical survey. *IEEE Access* **2020**, *8*, 47694–47712. [CrossRef]
85. Wu, C.; Gu, W.; Bo, R.; MehdipourPicha, H.; Jiang, P.; Wu, Z.; Lu, S.; Yao, S. Energy trading and generalized Nash equilibrium in combined heat and power market. *IEEE Trans. Power Syst.* **2020**, *35*, 3378–3387. [CrossRef]
86. Han, L.; Morstyn, T.; McCulloch, M.D. Scaling up cooperative game theory-based energy management using prosumer clustering. *IEEE Trans. Smart Grid* **2020**, *12*, 289–300. [CrossRef]
87. Wang, M.; Wu, Y.; Qin, S. Generalized nash equilibrium seeking for noncooperative game with different monotonicities by adaptive neurodynamic algorithm. *IEEE Trans. Neural Netw. Learn. Syst.* **2024**, *36*, 7637–7650. [CrossRef]
88. Liu, H.; Fan, A.; Li, Y.; Bucknall, R.; Chen, L. Hierarchical distributed MPC method for hybrid energy management: A case study of ship with variable operating conditions. *Renew. Sustain. Energy Rev.* **2024**, *189*, 113894.
89. Jafarzadeh, H.; Fleming, C. DMPC: A data-and model-driven approach to predictive control. *Automatica* **2021**, *131*, 109729.
90. Stanojev, O.; Markovic, U.; Aristidou, P.; Hug, G.; Callaway, D.; Vrettos, E. MPC-based fast frequency control of voltage source converters in low-inertia power systems. *IEEE Trans. Power Syst.* **2020**, *37*, 3209–3220.
91. Michailidis, P.; Michailidis, I.; Kosmatopoulos, E. Reinforcement learning for optimizing renewable energy utilization in buildings: A review on applications and innovations. *Energies* **2025**, *18*, 1724. [CrossRef]
92. Motalaei, S.; Khodabakhshian, M.; Majidi, F.A.; Abravesh, M. Optimizing Energy Efficiency in Educational Buildings Within a Hot-Arid Climate: Uncertainty and Sensitivity Analysis of Enclosed Interface Space Parameters. *J. Renew. Energy Environ.* **2026**, *13*, 58–66.
93. Jain, V.; Liu, S.; Iyer, G. Coping with Sample Inefficiency of Deep-Reinforcement Learning (DRL) for Embodied AI. 2020. Available online: https://vidhijain.github.io/pdfs/sample_inefficiency_in_DRL_for_embodied_AI.pdf (accessed on 2 March 2026).
94. Rajamallaiah, A.; Karri, S.P.K.; Alghaythi, M.L.; Alshammari, M.S. Deep reinforcement learning based control of a grid connected inverter with LCL-filter for renewable solar applications. *IEEE Access* **2024**, *12*, 22278–22295. [CrossRef]
95. Li, M.; Hu, D.; Lal, C.; Conti, M.; Zhang, Z. Blockchain-enabled secure energy trading with verifiable fairness in industrial Internet of Things. *IEEE Trans. Ind. Inform.* **2020**, *16*, 6564–6574. [CrossRef]
96. Wang, Z.-Y.; Chiang, H.-D. On the pseudo-bifurcation of non-convexity in the feasible region of AC optimal power flow. *IEEE Trans. Circuits Syst. II Express Briefs* **2022**, *69*, 2231–2235.
97. He, J.; Xiao, M.; Skoglund, M.; Poor, H.V. Straggler-resilient asynchronous ADMM for distributed consensus optimization. *IEEE Trans. Signal Process.* **2025**, *73*, 2496–2510. [CrossRef]
98. Yang, F.; Xie, X.; Sun, Q.; Yue, D. FDI attack estimation and event-triggered resilient control of DC microgrids under hybrid attacks. *IEEE Trans. Smart Grid* **2024**, *15*, 4207–4216. [CrossRef]
99. Herrera, M.; Pérez-Hernández, M.; Parlikad, A.K.; Izquierdo, J. Multi-agent systems and complex networks: Review and applications in systems engineering. *Processes* **2020**, *8*, 312. [CrossRef]
100. Bastianello, N.; Schenato, L.; Carli, R. A novel bound on the convergence rate of ADMM for distributed optimization. *Automatica* **2022**, *142*, 110403. [CrossRef]
101. Audrey, R.; ADEME; Charlotte, M.; Hélène, B.; Crédoc. *Revue de Littérature Sur Les Changements de Comportement Chez Les Autoconsommateurs Individuels, à la Suite de L'installation de Panneaux Photovoltaïques*; ADEME: Angers, France, 2026.
102. Simão, M.; Ramos, H.M. Hybrid pumped hydro storage energy solutions towards wind and PV integration: Improvement on flexibility, reliability and energy costs. *Water* **2020**, *12*, 2457. [CrossRef]
103. Skowroński, R. Liveness over Fairness (Part I): A Statistically Grounded Framework for Detecting and Mitigating PoW Wave Attacks. *Information* **2025**, *16*, 1060. [CrossRef]
104. Tan, R.; Li, R.; Yu, X.; Chen, X.; Xu, X.; Zhao, Z. Pareto actor-critic for communication and computation co-optimization in non-cooperative federated learning services. *IEEE Trans. Mob. Comput.* **2025**, *25*, 1628–1643.

105. Li, W.; Feng, C.; Zhang, L.; Xu, H.; Cao, B.; Imran, M.A. A scalable multi-layer PBFT consensus for blockchain. *IEEE Trans. Parallel Distrib. Syst.* **2020**, *32*, 1146–1160. [CrossRef]
106. Karniadakis, G.E.; Kevrekidis, I.G.; Lu, L.; Perdikaris, P.; Wang, S.; Yang, L. Physics-informed machine learning. *Nat. Rev. Phys.* **2021**, *3*, 422–440. [CrossRef]
107. Misyris, G.S.; Venzke, A.; Chatzivasileiadis, S. Physics-informed neural networks for power systems. In *2020 IEEE Power & Energy Society General Meeting (PESGM)*; IEEE: New York, NY, USA, 2020; pp. 1–5.
108. Barragán-Villarejo, M.; García-López, F.d.P.; Marano-Marcolini, A.; Maza-Ortega, J.M. Power system hardware in the loop (PSHIL): A holistic testing approach for smart grid technologies. *Energies* **2020**, *13*, 3858. [CrossRef]
109. Fuller, A.; Fan, Z.; Day, C.; Barlow, C. Digital twin: Enabling technologies, challenges and open research. *IEEE Access* **2020**, *8*, 108952–108971. [CrossRef]
110. Han, H.; Zhang, H.; Yang, J.; Su, H. Distributed model predictive consensus control for stable operation of integrated energy system. *IEEE Trans. Smart Grid* **2023**, *15*, 381–393. [CrossRef]
111. Alyas, T.; Abbas, Q.; Hayat, A.; Nawaz, W.; Alshanqiti, A.; Almoamari, H.; Ibrahim, A.M. Toward intelligent IoT scheduling with quantum-inspired latent models for energy and latency optimization. *Sci. Rep.* **2026**, *16*, 4234. [PubMed]
112. Zhou, Y.; Tajudin, N. Adaptive Manufacturing at Scale: Case Study on Digital Twin-Mas Synergy for Operational Excellence. *Sci. Conserv. Archaeol.* **2025**, *37*, 170–177.
113. Yu, W.; Patros, P.; Young, B.; Klinac, E.; Walmsley, T.G. Energy digital twin technology for industrial energy management: Classification, challenges and future. *Renew. Sustain. Energy Rev.* **2022**, *161*, 112407. [CrossRef]
114. Thakur, D.; Guzzo, A.; Fortino, G.; Piccialli, F. Green federated learning: A new era of green aware ai. *ACM Comput. Surv.* **2025**, *57*, 1–36. [CrossRef]
115. Nguyen, D.C.; Ding, M.; Pathirana, P.N.; Seneviratne, A.; Li, J.; Poor, H.V. Federated learning for internet of things: A comprehensive survey. *IEEE Commun. Surv. Tutor.* **2021**, *23*, 1622–1658.
116. Hudson, N.; Hossain, J.; Hosseinzadeh, M.; Khamfroush, H.; Rahnamay-Naeini, M.; Ghani, N. A framework for edge intelligent smart distribution grids via federated learning. In *2021 International Conference on Computer Communications and Networks (ICCCN)*; IEEE: New York, NY, USA, 2021; pp. 1–9.
117. Alghamedy, F.H.; El-Haggar, N.; Alsumayt, A.; Alfawaer, Z.; Alshammari, M.; Amouri, L.; Aljameel, S.S.; Albassam, S. Unlocking a Promising Future: Integrating Blockchain Technology and FL-IoT in the journey to 6G. *IEEE Access* **2024**, *12*, 115411–115447.
118. Gomes, J.; Khan, S.; Svetinovic, D. Fortifying the blockchain: A systematic review and classification of post-quantum consensus solutions for enhanced security and resilience. *IEEE Access* **2023**, *11*, 74088–74100. [CrossRef]
119. Cerezo, M.; Arrasmith, A.; Babbush, R.; Benjamin, S.C.; Endo, S.; Fujii, K.; McClean, J.R.; Mitarai, K.; Yuan, X.; Cincio, L.; et al. Variational quantum algorithms. *Nat. Rev. Phys.* **2021**, *3*, 625–644. [CrossRef]
120. Aleksis, R.; Pell, A.J. Low-power synchronous helical pulse sequences for large anisotropic interactions in MAS NMR: Double-quantum excitation of ^{14}N. *J. Chem. Phys.* **2020**, *153*, 244202. [PubMed]
121. Somvanshi, S.; Islam, M.; Chhetri, G.; Chakraborty, R.; Mimi, M.S.; Shuvo, S.A.; Islam, K.S.; Javed, S.; Rafat, S.A.; Dutta, A.; et al. From tiny machine learning to tiny deep learning: A survey. *ACM Comput. Surv.* **2025**, *58*, 1–33. [CrossRef]
122. Osman, A.; Abid, U.; Gemma, L.; Perotto, M.; Brunelli, D. Tinyml platforms benchmarking. In *International Conference on Applications in Electronics Pervading Industry, Environment and Society*; Springer International Publishing: Cham, Switzerland, 2021; pp. 139–148.
123. Gweon, S.; Kang, S.; Kim, K.; Yoo, H.-J. FlashMAC: A time-frequency hybrid MAC architecture with variable latency-aware scheduling for TinyML systems. *IEEE J. Solid-State Circuits* **2022**, *57*, 2944–2956.
124. Kluczek, A.; Żegleń, P.; Matušíková, D. The use of Prospect theory for energy sustainable industry 4.0. *Energies* **2021**, *14*, 7694. [CrossRef]
125. Kumar, S.; Datta, S.; Singh, V.; Datta, D.; Singh, S.K.; Sharma, R. Applications, challenges, and future directions of human-in-the-loop learning. *IEEE Access* **2024**, *12*, 75735–75760.
126. Andriopoulos, N.; Plakas, K.; Birbas, A.; Papalexopoulos, A. Design of a prosumer-centric local energy market: An approach based on prospect theory. *IEEE Access* **2024**, *12*, 32014–32032. [CrossRef]
127. Shi, M.; Shahidehpour, M.; Zhou, Q.; Chen, X.; Wen, J. Optimal consensus-based event-triggered control strategy for resilient DC microgrids. *IEEE Trans. Power Syst.* **2020**, *36*, 1807–1818.
128. Wang, D.; Gong, C.; Li, Y.; Ma, H.; Li, T.; Luo, S. Behaviorally Embedded Multi-Agent Optimization for Urban Microgrid Energy Coordination Under Social Influence Dynamics. *Energies* **2026**, *19*, 687. [CrossRef]
129. Xia, Y.; Wang, K.; Ji, H.; Wang, Q.; Shi, L.; Wu, F. Dynamic Network Usage Fee for Joint Kilowatt and Negawatt Peer-to-Peer Energy Market Based on Knowledge Distillation. *IEEE Trans. Smart Grid* **2025**, *17*, 2250–2264.
130. Doumen, S.C.; Hönen, J.; Nguyen, P.; Hurink, J.L.; Zwart, B.; Kok, K. Modeling and demonstrating the effect of human decisions on the distribution grid. In *2023 IEEE Power & Energy Society Innovative Smart Grid Technologies Conference (ISGT)*; IEEE: New York, NY, USA, 2023; pp. 1–5.

131. Mitchell Finnigan, S.J. Human-Centred Smart Buildings: Reframing Smartness Through the Lens of Human-Building Interaction. Ph.D. Thesis, Newcastle University, Newcastle upon Tyne, UK, 2020.
132. Iqbal, M.A. GRID MODERNIZATION: FROM TRADITIONAL TO AI-OPTIMIZED SELF-HEALING NETWORKS. *Spectr. Eng. Sci.* **2026**, *4*, 386–396.
133. Maurya, A.; Raju P, E.S.N. Self-Healing Schemes in Modern Advanced Power Distribution Networks: An Overview. In *2024 IEEE 11th Power India International Conference (PIICON)*; IEEE: New York, NY, USA, 2024; pp. 1–6.
134. Li, M.; Yu, F.R.; Si, P.; Wu, W.; Zhang, Y. Resource optimization for delay-tolerant data in blockchain-enabled IoT with edge computing: A deep reinforcement learning approach. *IEEE Internet Things J.* **2020**, *7*, 9399–9412.
135. Dandasi, V.V.; Gurubasannavar, S.D.; Sunku, R. Enhancing Smart Grid Security: A Multi-Criteria Evaluation Through GRA Method. *Int. J. Inf. Technol. Manag. Inf. Syst.* **2023**, *14*, 153–167. [CrossRef]
136. Guo, M.; De Persis, C.; Tesi, P. Data-driven stabilization of nonlinear polynomial systems with noisy data. *IEEE Trans. Autom. Control* **2021**, *67*, 4210–4217. [CrossRef]
137. Cavone, G.; Bozza, A.; Carli, R.; Dotoli, M. MPC-based process control of deep drawing: An industry 4.0 case study in automotive. *IEEE Trans. Autom. Sci. Eng.* **2022**, *19*, 1586–1598. [CrossRef]
138. Yao, Z.; Fang, Y.; Pan, H.; Wang, X.; Si, X. A secure and highly efficient blockchain PBFT consensus algorithm for microgrid power trading. *Sci. Rep.* **2024**, *14*, 8300. [CrossRef] [PubMed]
139. Chai, J.; Zhu, Y.; Zhao, D. NVIF: Neighboring variational information flow for cooperative large-scale multiagent reinforcement learning. *IEEE Trans. Neural Netw. Learn. Syst.* **2023**, *35*, 17829–17841. [CrossRef]
140. Mustafa, H.M.; Bariya, M.; Sajan, K.S.; Chhokra, A.; Srivastava, A.; Dubey, A.; von Meier, A.; Biswas, G. RT-METER: A real-time, multi-layer cyber-power testbed for resiliency analysis. In *Proceedings of the 9th Workshop on Modeling and Simulation of Cyber-Physical Energy Systems*; Association for Computing Machinery: New York, NY, USA, 2021; pp. 1–7.
141. Sudarsan, A.; Kurukkanari, C.; Bendi, D. A state-of-the-art review on readiness assessment tools in the adoption of renewable energy. *Environ. Sci. Pollut. Res.* **2023**, *30*, 32214–32229.
142. Ringelstein, J.; Marten, F.; Vogt, M.; Banerjee, G.; Bao, J. pandaict: A Novel Open-Source Tool for modeling Cyber-Physical Energy Systems. In *ETG Kongress 2025; Voller Energie—Heute und Morgen*; VDE: Frankfurt am Main, Germany, 2025; pp. 39–46.
143. Yao, Y.; Liu, W.; Jain, R.; Chowdhury, B.; Wang, J.; Cox, R. Quantitative metrics for grid resilience evaluation and optimization. *IEEE Trans. Sustain. Energy* **2022**, *14*, 1244–1258. [CrossRef]
144. Xu, J.; Gao, H.; Wang, R.; Liu, J. Real-time operation optimization in active distribution networks based on multi-agent deep reinforcement learning. *J. Mod. Power Syst. Clean Energy* **2023**, *12*, 886–899. [CrossRef]
145. Dolev, D.; Reischuk, R.; Schneider, F.B.; Strong, H.R. *Time Services (Dagstuhl Seminar 9611)*; Schloss Dagstuhl-Leibniz-Zentrum für Informatik: Wadern, Germany, 2021.
146. Dawson, C.; Gao, S.; Fan, C. Safe control with learned certificates: A survey of neural lyapunov, barrier, and contraction methods for robotics and control. *IEEE Trans. Robot.* **2023**, *39*, 1749–1767. [CrossRef]
147. Luo, H.; Yang, X.; Yu, H.; Sun, G.; Lei, B.; Guizani, M. Performance analysis and comparison of nonideal wireless PBFT and RAFT consensus networks in 6G communications. *IEEE Internet Things J.* **2023**, *11*, 9752–9765. [CrossRef]
148. Reif, V.; Strasser, T.I.; Jimeno, J.; Farre, M.; Genest, O.; Gyrard, A.; McGranaghan, M.; Lipari, G.; Schütz, J.; Uslar, M.; et al. Towards an interoperability roadmap for the energy transition. *Elektrotech. Inf.* **2023**, *140*, 478–487. [CrossRef]
149. de Jesus, V.S.; Lazarin, N.M.; Pantoja, C.E.; Manoel, F.C.P.B.; Alves, G.V.; Viterbo, J. A middleware for providing communicability to Embedded MAS based on the lack of connectivity. *Artif. Intell. Rev.* **2023**, *56*, 2971–3001. [CrossRef]
150. Devarajan, G.; Kumar, P.N.; Chinnusamy, M.; Kanagaraj, S.; Chenniappan, S. Modeling and simulation of smart power systems using hil. In *Artificial Intelligence-Based Smart Power Systems*; Wiley-IEEE Press: Hoboken, NJ, USA, 2023; pp. 291–309.
151. Bennetot, A.; Donadello, I.; Haouari, A.E.Q.E.; Dragoni, M.; Frossard, T.; Wagner, B.; Sarranti, A.; Tulli, S.; Trocan, M.; Chatila, R.; et al. A practical tutorial on explainable AI techniques. *ACM Comput. Surv.* **2024**, *57*, 1–44. [CrossRef]
152. Cifci, A. Interpretable prediction of a decentralized smart grid based on machine learning and explainable artificial intelligence. *IEEE Access* **2025**, *13*, 36285–36305. [CrossRef]
153. Stepanova, A.I.; Khalyasmaa, A.I.; Matrenin, P.V.; Eroshenko, S.A. Application of SHAP and Multi-Agent Approach for Short-Term Forecast of Power Consumption of Gas Industry Enterprises. *Algorithms* **2024**, *17*, 447.
154. Virgili, M.; Babu, N.; Javidsharifi, M.; Valiulahi, I.; Masouros, C.; Forsyth, A.J.; Kerekes, T.; Papadias, C.B. Cost-efficient design of an energy-neutral UAV-based mobile network. *IEEE Trans. Commun.* **2022**, *70*, 6890–6901.
155. Zhang, T.; Chen, W. Computation offloading in heterogeneous mobile edge computing with energy harvesting. *IEEE Trans. Green Commun. Netw.* **2021**, *5*, 552–565. [CrossRef]
156. Chen, P.; Liu, S.; Wang, X.; Kamwa, I. Physics-guided multi-agent deep reinforcement learning for robust active voltage control in electrical distribution systems. *IEEE Trans. Circuits Syst. I Regul. Pap.* **2023**, *71*, 922–933.
157. Shi, N.; Cheng, R.; Liu, L.; Wang, Z.; Zhang, Q.; Reno, M.J. Data-driven affinely adjustable robust Volt/VAr control. *IEEE Trans. Smart Grid* **2023**, *15*, 247–259.

158. Zhu, J.; Liu, Z.; Dai, F.; Ou, W.; Jiao, Y.; Xiang, Y. Coordinated Planning of Unbalanced Flexible Interconnected Distribution Networks Based on Distributed Optimization. *Energies* **2026**, *19*, 1769. [CrossRef]
159. Huang, H.; Camlibel, M.K.; Carloni, R.; van Waarde, H.J. Feedback Stabilization of Polynomial Systems: From Model-based to Data-driven Methods. *IEEE Trans. Autom. Control* **2026**, 1–8. [CrossRef]
160. Liu, K.; Zheng, J.; Zhao, S. Fixed-Time Multi-UAV Collaborative Fault-Tolerant Formation Control for Sensor/Actuator Faults. In *2024 IEEE 63rd Conference on Decision and Control (CDC)*; IEEE: New York, NY, USA, 2024; pp. 2062–2067.